

Chiral Polaritonics: Analytic Solutions, Intuition and its Use

Christian Schäfer^{*,†} and Denis G. Baranov^{*,‡}

[†]*MC2 Department, Chalmers University of Technology, Sweden*

[‡]*Center for Photonics and 2D Materials, Moscow Institute of Physics and Technology, Dolgoprudny 141700, Russia*

E-mail: christian.schaefer.physics@gmail.com; denis.baranov@phystech.edu

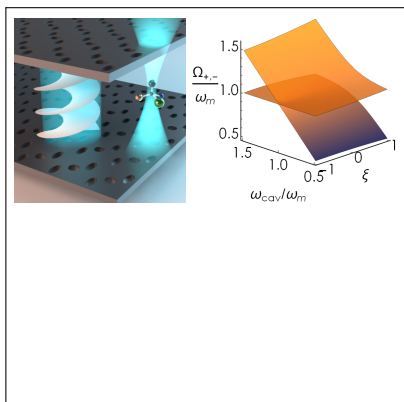
Abstract

Preferential selection of a given enantiomer over its chiral counterpart becomes increasingly relevant in the advent of the next era of medical drug design. In parallel, cavity quantum electrodynamics has grown into a solid framework to control energy transfer and chemical reactivity. In this work, we derive an analytical solution to a system of many chiral emitters interacting with a chiral cavity – in analogy to the widely used Tavis-Cummings and Hopfield models of quantum optics. We are able to estimate the discriminating strength of chiral polaritonics, discuss possible future development directions, exciting applications such as elucidating homochirality, and deliver much needed intuition to foster the freshly flourishing field of chiral polaritonics.

Keywords

Chiral Polaritonics, Strong Coupling, Polaritons, Optical Cavities, Resonances, Chirality, Handedness

Graphical TOC Entry



arXiv:2209.07177v2 [quant-ph] 31 Jan 2023

Coupling between two harmonic oscillators, either of classical or quantum origin, leads to a hybridization and the creation of new quasi-particle states if the coupling strength exceeds all the decay and decoherence rates in the combined system. A common representative for such a system is the interaction between an energetically isolated electromagnetic mode and a set of quantum emitters such as molecules. The associated quasi-particle states are referred to as polaritons and possess mixed light and matter characteristics which opens a toolbox with enormous versatility.¹⁻¹⁵ Polaritons of various flavours have been used or proposed as path to enhanced charge and excitation transfer,¹⁶⁻²² modify chemical reactivity,²³⁻³⁸ and alter a systems state and response to external stimuli,³⁹⁻⁴⁷ to name only a few.

So far, most experimental and theoretical efforts in this field have focused on coupling optical cavities with either linearly- or circularly-polarized electronic transitions of various quantum emitters. This is perfectly justified by the fact that in the visible and infrared ranges the interaction of light with electronic and vibrational transitions is dominated by the electric dipole term of the Hamiltonian. Nevertheless, there are examples of media that exhibit resonances with non-negligible magnetic transition dipole moment. One such practically relevant example is presented by the class of *chiral* media.⁴⁸⁻⁵⁰

A geometrical shape in three-dimensional space is called chiral if it cannot be aligned with its mirror image by a series of rotations and translations.⁵¹ The chirality occurs at various scales ranging from the shapes of galaxies down to drug and bio-molecules. Especially the latter receives a steady stream of attention in the ongoing quest for new, safer and affordable ways to design chemical complexes and drugs.^{52,53} It is then intuitively pivotal for its success to develop a solid understanding of relevant processes and a wide range of readily usable techniques that allow a separation or discrimination of the two enantiomers of a chiral structure.

While the recent years showed major progress in this field,^{54,55} sometimes referred to as chiral recognition, widely used chemical strate-

gies such as (re)crystallization⁵⁶ can be cumbersome and require often highly specified approaches for each individual compound. Interaction of chiral matter with circularly polarized electromagnetic fields leads to the effect of circular dichroism, which underlies numerous methods for distinguishing molecular enantiomers.⁵⁷ However, those interactions are usually *weak* and can be well understood without the need to consider a correlated motion between light and matter. If and how *strong* light-matter interaction can aid those challenging tasks remained largely unclear thus far.

While chiral polaritonics is still in its infancy, recent theoretical work is beginning to explore this question. Mauro et al. investigated the optical features of a single-handedness cavity loaded with a Pasteur medium using classical electromagnetism.⁵⁸ Riso et al. studied changes in the correlated ground state of single (or few) realistic molecules minimally coupled to an amplified chiral mode.⁵⁹

In this letter, we provide an analytic solution and much needed intuition that will be of good use for the future development of chiral polaritonics. Starting from non-relativistic quantum electrodynamics (QED), we derive the quantized electromagnetic fields supported by a single-handedness chiral cavity⁶⁰ and couple them to a large set of chiral emitters as illustrated in Fig. 1. The resulting Hamiltonian can serve as starting point for any kind of *ab initio* QED.^{13,61-65} Here, we focus on a simplified model that allows for an analytic solution which illustrates the physical playground, potential, and forthcoming challenges of chiral polaritonics. In contrast to previous approaches,^{54,55,66-68} the strong coupling to a chiral cavity allows one to reach sizeable interaction strength even in the absence of any pumping field. The here derived model paves the way to invigorate an entirely new research domain.

We start our derivation from the non-relativistic and spin-less limit of QED in Coulomb gauge. Using the Power-Zienau-Wooley transformation and expanding the multi-polar light-matter interaction to second order introduces magnetic dipolar couplings

and electric quadrupole terms^{69–72} according to

$$\hat{H} = \hat{H}_M + \hat{H}_L + \hat{H}_{LM},$$

where we differentiate between the N_M electronic ($q_i = -e$) and nuclear ($q_i = eZ_i$) charges plus longitudinal Coulomb interaction among them constituting the molecule, and inter-molecular Coulomb interactions

$$\hat{H}_M = \sum_{n=1}^N \sum_{i=1}^{N_M} \frac{1}{2m_i} \hat{\mathbf{p}}_{i,n}^2 + \sum_{n=1}^N \hat{V}_{\parallel}^n(\hat{\mathbf{r}}) + \sum_{n \neq n'}^N \hat{V}_{\parallel}^{n,n'}(\hat{\mathbf{r}}),$$

$$\hat{H}_L = \frac{1}{2} \int d^3\mathbf{r} \left[\frac{\hat{\mathbf{D}}_{\perp}^2(\mathbf{r})}{\varepsilon_0} + \varepsilon_0 c^2 \hat{\mathbf{B}}^2(\mathbf{r}) \right].$$

The interaction H_{LM} up to magnetic order takes the form

$$\begin{aligned} \hat{H}_{LM} = & -\frac{1}{\varepsilon_0} \sum_n \hat{\boldsymbol{\mu}}_n \cdot \hat{\mathbf{D}}_{\perp}(\mathbf{r}_n) - \sum_n \hat{\mathbf{m}}_n \cdot \hat{\mathbf{B}}(\mathbf{r}_n) \\ & - \frac{1}{\varepsilon_0} \sum_n \sum_{a,b \in \{x,y,z\}} \hat{Q}_{ab,n} \nabla_{a,n} \hat{D}_{\perp,b}(\mathbf{r}_n) \quad (1) \\ & + \frac{1}{8m} \sum_{n,i} (q_{n,i} \hat{\mathbf{r}}_{n,i} \times \hat{\mathbf{B}}(\mathbf{r}_n))^2 + \frac{1}{2\varepsilon_0} \int d^3\mathbf{r} \hat{\mathbf{P}}_{\perp}^2, \end{aligned}$$

with the canonical particle momentum $\mathbf{p}_i = m_i \dot{\mathbf{r}}_i - \frac{q_i}{2} \mathbf{r}_i \times \mathbf{B}(\mathbf{r})$, the total transverse polarization $\hat{\mathbf{P}}_{\perp} = \sum_n \hat{\mathbf{P}}_{\perp,n}$, the electric dipole moment $\hat{\boldsymbol{\mu}} = \sum_i q_i \hat{\mathbf{r}}_i$ and quadrupole Q_{ab} , as well as the magnetic dipole $\hat{\mathbf{m}} = \frac{1}{2} \sum_i \frac{q_i}{m_i} \hat{\mathbf{r}}_i \times \hat{\mathbf{p}}_i$. All positions are defined relative to each individual molecular center of mass. Importantly, the multi-polar form introduces the displacement field $\hat{\mathbf{D}}_{\perp} = \varepsilon_0 \hat{\mathbf{E}} + \hat{\mathbf{P}}$ as the canonical momentum to the vector potential. The last term in Eq. (1) can be written in the tensorial form $\sum_n \hat{\chi}_{n,ij}^m \hat{B}_i(\mathbf{r}_n) \hat{B}_j(\mathbf{r}_n)$ with $\hat{\chi}_{n,ij}^m = \sum_a q_a^2 / 8m_a (\hat{r}_{n,a}^{(i)} \hat{r}_{n,a}^{(j)} - \hat{r}_{n,a}^{(j)} \hat{r}_{n,a}^{(i)})$.

Let us briefly comment on the relevance of the appearing self-interaction contributions. The magnetic $\sum_n \hat{\chi}_{n,ij}^m \hat{B}_i(\mathbf{r}_n) \hat{B}_j(\mathbf{r}_n)$ and electric $\frac{1}{2\varepsilon_0} \int d^3\mathbf{r} \hat{\mathbf{P}}_{\perp}^2$ self-polarization terms ensure gauge invariance and guarantee the stability of the correlated system.^{70,73} A common simplification is to assume the molecules as well separated. In this dilute limit and when *all* photonic modes are considered, the inter-

molecular Coulomb interactions cancel perturbatively with the inter-molecular contributions arising from $\frac{1}{2\varepsilon_0} \int d^3\mathbf{r} \sum_{n,n'} \hat{\mathbf{P}}_{\perp,n} \hat{\mathbf{P}}_{\perp,n'}$ such that only retarded intermolecular interactions via the photonic fields remain.^{70,74} However, when the number of photonic modes is truncated, as commonly done for polaritonic systems, this intuitive result does no longer hold. If the intermolecular contributions are neglected nevertheless, one arrives at the widely used Dicke model that falsely predicts a transition into a superradiant phase, while the associated model in the Coulomb gauge does not exhibit such a transition.⁷⁵ Under which conditions a phase-transition for more realistic systems could appear and what characterizes such a transition is still a matter of active debate.^{42,76–80} We provide a derivation in analogy to the common Dicke model in the SI and focus in the following on the development of a non-perturbative chiral model.

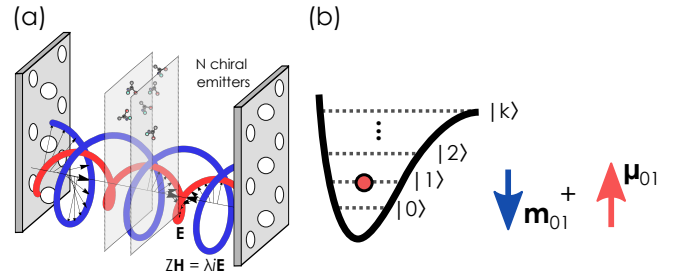


Figure 1: (a) Illustration of the system under study. N identical chiral (quantum) emitters interact with the electromagnetic field of a chiral standing wave. A chiral standing wave is formed between two handedness-preserving metasurface mirrors. (b) A model of a single chiral emitter as generic N -level system. Chiral emitters, which represent molecules, biological structures or plasmonic meta-atoms, are modeled as simplified multi-level systems whose transitions are quantified by collinear electric and magnetic dipole moments.

The electromagnetic fields follow the generic

mode expansion

$$\hat{\mathbf{D}}_{\perp}(\mathbf{r}) = i \sum_{\mathbf{k}, \lambda} \sqrt{\frac{\hbar c k \epsilon_0}{2V}} (\epsilon_{\mathbf{k}\lambda} e^{i\mathbf{k}\cdot\mathbf{r}} \hat{a}_{\mathbf{k}\lambda} - \epsilon_{\mathbf{k}\lambda}^* e^{-i\mathbf{k}\cdot\mathbf{r}} \hat{a}_{\mathbf{k}\lambda}^{\dagger}),$$

$$\hat{\mathbf{B}}(\mathbf{r}) = i \frac{1}{c} \sum_{\mathbf{k}, \lambda} \sqrt{\frac{\hbar c k}{2\epsilon_0 V}} (\beta_{\mathbf{k}\lambda} e^{i\mathbf{k}\cdot\mathbf{r}} \hat{a}_{\mathbf{k}\lambda} - \beta_{\mathbf{k}\lambda}^* e^{-i\mathbf{k}\cdot\mathbf{r}} \hat{a}_{\mathbf{k}\lambda}^{\dagger})$$

where V is the cavity mode volume, $\epsilon_{\mathbf{k},\lambda}$ and $\beta_{\mathbf{k},\lambda}$ are the electric and magnetic field unit polarization vectors; \mathbf{k} labels wave vectors, and λ labels polarization states.

Although Maxwell's equations in free space admit solutions in the form of chiral photons, in this case both handednesses coexist at the same time. Contrary to one's intuition, illuminating an ordinary Fabry-Pérot cavity with a circularly polarized light does not address this problem.^{13,81} However, using cleverly designed asymmetric "single-handedness" cavities,^{60,82} it is possible to engineer pure chiral electromagnetic fields with only one handedness. In a right-handed (left-handed) monochromatic wave the magnetic field is $\pi/2$ behind (ahead) the electric field everywhere in space $Z\mathbf{H}(\mathbf{r};\omega) = -i\lambda\mathbf{E}(\mathbf{r};\omega)$, where $Z = \sqrt{\mu_0/\epsilon_0}$ is the impedance of free space, and λ is the eigenvalue of the helicity operator,⁸³ which takes values $+1$ and -1 for LH and RH fields, respectively. Only a subset of modes will adhere to the conditions that are imposed by the boundary conditions of the chiral cavity, it should be noted that the electromagnetic fields are not zero at the mirror-surfaces.

A planar optical cavity, such as the one described in Ref.,⁶⁰ supports a continuous spectrum of resonant states that can be labels by their in-plane momenta \mathbf{k}_{\parallel} . Cavity fields maintain their single-handedness quality for a substantial range of in-plane wave vectors (incident angles).⁶⁰ For simplicity, we will illustrate only coupling of a single standing wave with $\mathbf{k}_{\parallel} = 0$ to the chiral emitters, and refer the interested reader to the SI for a generalized discussion. The chiral standing wave is the superposition of two counter-propagating circularly polarized plane waves of the same handedness. Assuming the axis of the cavity to be pointed along the z direction and considering a vertical stand-

ing wave with $\mathbf{k} = \pm k\mathbf{e}_z$, the displacement field $\hat{\mathbf{D}}_{\perp}^{\lambda}(\mathbf{r}) = \sum_{\mathbf{k}, \lambda} \hat{\mathbf{D}}_{\mathbf{k}, \pm}^{\lambda}(\mathbf{r})$ of a LH/RH standing wave is $\hat{\mathbf{D}}_{\perp}^{\lambda}(\mathbf{r}) = (\hat{\mathbf{D}}_{+k, \pm}^{\lambda}(\mathbf{r}) + \hat{\mathbf{D}}_{-k, \pm}^{\lambda}(\mathbf{r}))/\sqrt{2}$ with $\hat{a}_{+k, \lambda} = \hat{a}_{-k, \lambda}$ and $\epsilon_{\pm k, \lambda} = \frac{1}{\sqrt{2}}(1, \pm i\lambda, 0)^T$.

With these simplifications, the displacement field of a chiral standing waves takes the form

$$\hat{\mathbf{D}}_{\perp}^{\lambda}(\mathbf{r}) = -\sqrt{\frac{\epsilon_0}{V}} \tilde{\varepsilon}_k^{\lambda}(z) \hat{p}_{k, \lambda},$$

where $\tilde{\varepsilon}_k^{\lambda}(z) = (\cos(kz), -\lambda \sin(kz), 0)^T$ is the z -dependent polarization vector of the chiral standing wave, and the canonical coordinates are $\hat{p}_{k, \lambda} = -i\sqrt{\hbar c k/2}(\hat{a}_{k, \lambda} - \hat{a}_{k, \lambda}^{\dagger})$ and $\hat{q}_{k, \lambda} = \sqrt{\hbar/2ck}(\hat{a}_{k, \lambda} + \hat{a}_{k, \lambda}^{\dagger})$. Notice that the left- and right-handed polarization vectors are orthogonal only in the spatially averaged sense. Recalling the relation between the electric and magnetic field of a chiral field, $\beta_{\mathbf{k}, \lambda} = -i\lambda\epsilon_{\mathbf{k}, \lambda}$, we obtain the magnetic field of a chiral standing wave as $\hat{\mathbf{B}}_{\lambda}(\mathbf{r}) = \sqrt{k^2/\epsilon_0 V} \lambda \tilde{\varepsilon}_k^{\lambda}(z) \hat{q}_{k, \lambda}$.

The standing chiral fields satisfy Maxwell's equation and contribute with $ck = \omega_k$ a photonic energy of $\hat{H}_L = (\hat{p}_k^2 + \omega_k^2 \hat{q}_k^2)/2 = \hbar\omega_k(\hat{a}_k^{\dagger} \hat{a}_k + \frac{1}{2})$ for a given handedness. The extraordinary consequence is now that the standing field in an empty cavity will feature chiral quantum-fluctuations, i.e., for each Fock-state $|n\rangle$ the optical chirality density $C_n(\mathbf{r}, \omega) = \frac{\epsilon_0 \omega}{2} \Im \langle n | \hat{\mathbf{E}} \cdot \hat{\mathbf{B}}^* | n \rangle$ reduces to $C_n(\mathbf{r}, \omega) = \lambda \hbar \omega_k k / 4V$. Also a dark chiral cavity will influence the ground and excited states of matter located within it. In the following, we will introduce a series of simplifications and derive an analytic solution to the combined system of many chiral molecules coupled to the chiral cavity.

Let us here briefly describe the derivation of the analytical solution and their underlying models, a detailed version can be found in the SI. For negligible intermolecular Coulombic interactions, i.e., $\hat{V}_{\parallel}^{n, n'} \approx 0$, the molecular component to the Hamiltonian becomes diagonal $\hat{H}_M = \sum_{n=1}^N \sum_{k=1}^{\infty} E_k^n |k_n\rangle \langle k_n|$ in the many-body eigenstates $|k\rangle$. Expanding all transition elements in this eigenbasis would, in principle, allow for a numerical solutions of the (ultra-)strongly coupled system. The inter-

ested reader might refer to the area of *ab initio* QED.⁸⁴ Here, we focus on simplified models that provide analytical solutions.

The self-magnetization term mediated via $\hat{\chi}_{n,ij}^m$ will be assumed to be purely parametric $\hat{\chi}_{n,ij}^m \approx \chi_{n,ij}^m$ as it obstructs otherwise the Hopfield diagonalization scheme. The self-magnetization ensures gauge invariance and should be expected to play an important role for more sophisticated *ab initio* approaches. We define the dressed photonic frequency $\bar{\omega}_k^2 = \omega_k^2 [1 + 2 \sum_n \sum_{i,j=1}^3 \chi_{n,ij}^m \bar{\varepsilon}_{k,i}^\lambda(z) \bar{\varepsilon}_{k,j}^\lambda(z) / (c^2 \varepsilon_0 V)]$ which is related via the sum-rule $\bar{\omega}_k^2 = 2 \sum_n (E_n - E_m) / \hbar^2 |\langle m | \hat{p}_k | n \rangle|^2 \quad \forall m$ to the eigenvalues E_m and eigenstates $|m\rangle$.

In order to provide analytical solutions, we will limit our selves in the following to *either* two-level systems $\hat{\boldsymbol{\mu}}_n \rightarrow (\boldsymbol{\mu}_{10}^n \hat{\sigma}_+ + \boldsymbol{\mu}_{01}^n \hat{\sigma}_-)$ or harmonic oscillators $\hat{\boldsymbol{\mu}}_n \rightarrow (\boldsymbol{\mu}^{n,*} \hat{b}^\dagger + \boldsymbol{\mu}^n \hat{b})$. Both approaches are widely used but we will focus ultimately on the harmonic representation as it allows to access non-perturbative correlation in the analytic solution. Our molecules are neutral such that we disregard permanent dipole moments for brevity.

The relationship between the transition dipole moments has the generic form $\mathbf{m}_{01}^n = \overset{\leftrightarrow}{\xi} \boldsymbol{\mu}_{01}^n$, where ξ is the product of a 3D rotation and scaling (see SI). For brevity, we are going to limit our analysis to molecules with collinear transition dipole moments and refer the reader to the SI for a generalization. In this scalar case, $\xi = +1$ and $\xi = -1$ describe an ideal LH and RH emitter, respectively.⁵⁰ This allows us to combine electric dipole, electric quadrupole and magnetic dipole into a single compact expression when $\boldsymbol{\mu}_{10}^n = \boldsymbol{\mu}_{01}^n$ and $Q_{ab,n}^{10} = Q_{ab,n}^{01}$, $\mathbf{Q}_n = Q_{ab,n}^{10} \nabla_a \mathbf{e}_b$. From here on, we are left to follow two different but equally popular directions that we detail in the following.

A convenient and widely used approximation in quantum optics is to assume that the molecular basis consists of merely two states, motivated by the anharmonicity of excitonic transitions. For very large coupling strength, there is little reason to believe that the complicated multi-level structure of chiral molecules is well

captured by only a single excitation. Let us assume for a moment we would limit ourselves to this parameter regime. The excitation spectrum is then approximated by a single excitation of energy $\hbar\omega_m$ which is commonly transferred into a Pauli spin-basis $|1\rangle\langle 0| \rightarrow \sigma^+$. If we further discard the self-polarization term and counter-rotating terms ($\hat{a}\hat{\sigma}^-$, $\hat{a}^\dagger\hat{\sigma}^+$), we obtain the strongly simplified chiral Tavis-Cummings Hamiltonian

$$\hat{H}_{CTC} = \sum_n \hbar\omega_m \hat{\sigma}_n^+ \hat{\sigma}_n^- + \hbar\bar{\omega}_k (\hat{a}^\dagger \hat{a} + \frac{1}{2}) - i\hbar \sum_n \bar{g}_n (1 + \bar{\xi}_n \lambda) [\hat{\sigma}_n^+ \hat{a} - \hat{\sigma}_n^- \hat{a}^\dagger] .$$

The chiral coupling is encoded via the effective interaction strength proportional to $\bar{g}_n (1 + \bar{\xi}_n \lambda)$. A chiral emitter that features the same (opposite) handedness as the cavity will couple stronger (weaker) to the mode. In the extreme case that $\bar{\xi}_n = \pm 1$, the mismatched enantiomer will entirely decouple from the mode. The above chiral Tavis-Cummings model can be solved analogously to the standard Tavis-Cummings model, i.e, by limiting ourselves to the single-excitation subspace and introducing collective spin-operators.

Once we approach the ultra-strong coupling domain, many excitations of the chiral molecule will contribute to the renormalization of transitions. A possible alternative is the harmonic approximation, in analogy to Hopfield,⁸⁵ in which we identify the excitation structure with that of an harmonic oscillator. The resulting Hamiltonian takes the form of $N + 1$ coupled harmonic oscillators and can be solved via Hopfield diagonalization (detailed in the SI). The Hopfield solution is known to provide accurate predictions for effectively bosonic systems, such as vibrations⁸⁶ and intersubband transitions.⁸⁷ We find that the qualitative predictions of our Hopfield model are consistent with available *ab initio* calculations (see SI and following). It should be noted that both models provide consistent predictions for the first polariton-manifold under strong coupling as $\hat{\sigma}_+ \leftrightarrow \hat{b}^\dagger$ in the single-excitation space.

Assuming identical (but distinguishable)

molecules and homogeneous in-plane distribution, it is convenient to introduce collective molecular operators $\hat{B}_{\mathbf{k}_{\parallel}}^{\dagger} = \frac{1}{\sqrt{N}} \sum_n e^{i\mathbf{k}_{\parallel} \cdot \mathbf{r}_n} \hat{b}_n^{\dagger}$, $\hat{b}_n^{\dagger} = \frac{1}{\sqrt{N}} \sum_{\mathbf{k}_{\parallel}} e^{-i\mathbf{k}_{\parallel} \cdot \mathbf{r}_n} \hat{B}_{\mathbf{k}_{\parallel}}^{\dagger}$, where \mathbf{k}_{\parallel} is the in-plane momentum of the matter excitation. The general feature of chiral selectivity is unchanged (see SI). Under those approximations

$$\begin{aligned} \hat{H} \approx & \hbar\tilde{\omega}_m (\hat{B}_{k=0}^{\dagger} \hat{B}_{k=0} + \frac{1}{2}) + \hbar\tilde{\omega}_k (\hat{a}^{\dagger} \hat{a} + \frac{1}{2}) \\ & - i\hbar\sqrt{N}\tilde{g} [(\hat{B}_{k=0}^{\dagger} + \hat{B}_{k=0})(\hat{a} - \hat{a}^{\dagger}) \\ & + \tilde{\xi}\lambda(\hat{B}_{k=0}^{\dagger} - \hat{B}_{k=0})(\hat{a} + \hat{a}^{\dagger})], \end{aligned} \quad (2)$$

where $\tilde{\omega}_m^2 = \omega_m^2 + N(2\omega_m/\hbar\varepsilon_0 V)(\tilde{\varepsilon}_k^{\lambda}(z) \cdot \boldsymbol{\mu})^2$, $\tilde{g} = \sqrt{\hbar\tilde{\omega}_k\omega_m/(2\varepsilon_0 V\tilde{\omega}_m)}(\boldsymbol{\mu} + \mathbf{Q}) \cdot \tilde{\varepsilon}_k^{\lambda}(z)$ and $\tilde{\xi} = \xi\tilde{\omega}_m\omega_k\boldsymbol{\mu} \cdot \tilde{\varepsilon}_k^{\lambda}(z)/(\omega_m\tilde{\omega}_k(\boldsymbol{\mu} + \mathbf{Q}) \cdot \tilde{\varepsilon}_k^{\lambda}(z))$ are the renormalized effective excitation energy, coupling strength, and chirality factor.

Eq. (2) is diagonalized by following the standard Hopfield^{85,87} procedure, i.e., defining the polaritonic operator $\hat{\Pi} = x\hat{a} + y\hat{a}^{\dagger} + z\hat{B}_{k=0} + u\hat{B}_{k=0}^{\dagger}$ that fulfills the eigenvalue equation $[\hat{H}, \hat{\Pi}] = \hbar\Omega\hat{\Pi}$ with the normalization condition $|x|^2 - |y|^2 + |z|^2 - |u|^2 = 1$. We obtain the polaritonic frequencies as real and positive solutions

$$\begin{aligned} \Omega_{\pm} = & \frac{1}{\sqrt{2}} \left\{ \tilde{\omega}_k^2 + \tilde{\omega}_m^2 + 8\tilde{\xi}\lambda N\tilde{g}^2 \pm \left[(\tilde{\omega}_k^2 - \tilde{\omega}_m^2)^2 \right. \right. \\ & \left. \left. + 16N\tilde{g}^2(\tilde{\omega}_k + \tilde{\omega}_m\tilde{\xi}\lambda)(\tilde{\omega}_k\tilde{\xi}\lambda + \tilde{\omega}_m) \right]^{\frac{1}{2}} \right\}^{\frac{1}{2}}, \end{aligned} \quad (3)$$

with eigenvalues $E_{\pm} = \hbar\Omega_{\pm} + E_{vac}$, $E_{vac} = \hbar(\Omega_+ + \Omega_-)/2$ up to an arbitrary constant that is independent of the handedness of the emitter.

As illustrated in Fig. 2(a), an ensemble of ideal chiral emitters featuring the opposite handedness ($\tilde{\xi}\lambda = -1$) compared to the LH cavity mode effectively decouples from the cavity. Switching the cavity handedness would therefore allow to open and close the avoided crossing and control associated conical intersections. This is an intuitively expected result: an ensemble of LH molecules couples to the LH photonic mode, whereas an ensemble of equivalent RH molecules becomes transparent for the same optical mode. The cross-section of the full plot at $\xi = 0$ yields the familiar picture

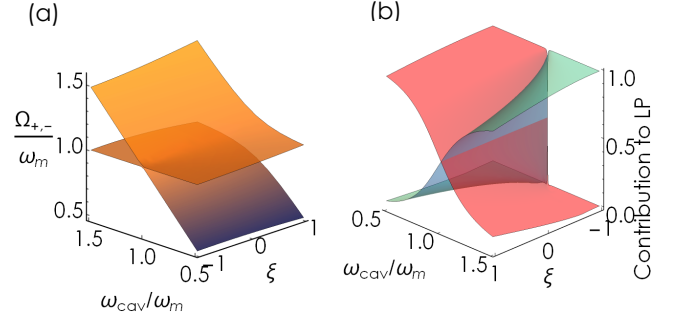


Figure 2: (a) Polaritonic eigenvalues Ω_{\pm} of the chiral Hopfield model with a LH cavity mode ($\lambda = 1$) for $N = 100$ as a function of the cavity frequency ω_k and chiral factor ξ . The eigenvalues are calculated with typical values for optical transitions in dye molecules,⁵⁷ $\mathbf{Q} = \chi_{i,j}^m = z = 0$, and the fundamental coupling strength of $\sqrt{1/\varepsilon_0 V} = 0.001$ (a.u.). (b) Hopfield coefficients (light blue – photonic, red – matter) for the lower polariton for the same system as in panel (a).

of ”traditional” polaritons with the electric-dipole-mediated coupling.⁸⁷ Furthermore, the photonic and matter polariton fractions exhibit a gradual transition from the regime of hybridized eigenstates at $\tilde{\xi}\lambda = 1$ to the uncoupled regime at $\tilde{\xi}\lambda = -1$, when the two eigenstates represent bare optical and matter excitations. Our simple Hopfield solution recovers therefore the promising feature that the vacuum coupling in chiral cavities can be used to discriminate between two enantiomers. Importantly, the cavity distinguishes only the chiral component, i.e., the parallel projection of $\boldsymbol{\mu}$. This can be easily seen by extending our discussion to consider general bi-isotropic media and performing an angular average (see SI).

The vast majority of widely used molecular systems exhibits extremely weak chirality factors $\xi \ll 1$, rendering it challenging to separate left- and right-handed enantiomers to high fidelity. Chiral polaritonics can serve this purpose as the collective interaction results in a \sqrt{N} scaling of the coupling strength, thus increasing the selectivity. Fig. 3 illustrates the difference of upper and lower polaritonic eigenfrequencies (blue) between left- and right-handed enantiomer for typical dye molecules⁵⁷ with a small and conservative estimate of $\xi \approx$

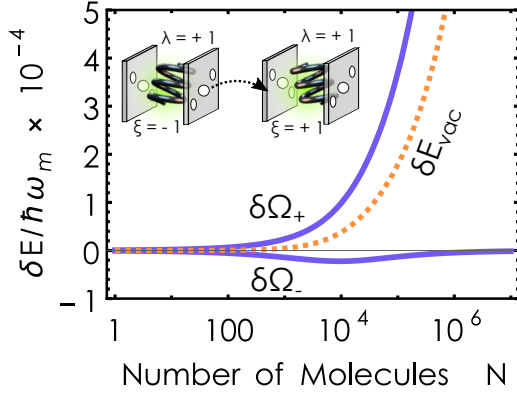


Figure 3: Normalized difference between the polaritonic excitation energies $\delta\Omega_{\pm} = \Omega_{\pm}^{\xi=+1} - \Omega_{\pm}^{\xi=-1}$ (blue-solid) and the correlated ground state $\delta E_{vac} = E_{vac}^{\xi=+1} - E_{vac}^{\xi=-1}$ (orange-dotted) of left and right-handed chiral dye molecules inside a LH chiral cavity. We have chosen common values for dye molecules,⁵⁷ the resonant condition $\omega_k = \omega_m$ and $\sqrt{1/\epsilon_0 V} = 0.001$ in atomic units for the chiral Hopfield model. For comparison, a molecular concentration of 1 mol/L is on the order of magnitude of 10^3 molecules in the chosen volume. The actual number of collectively coupled emitters under experimental conditions is usually unknown and is estimated based on simplified models, such as the one presented here.

$3.712 \cdot 10^{-5}$ for the chirality factor.

For large N , the interacting system enters into the ultra-strong coupling domain in which the combined light-matter ground state is no longer separable. The relative energy difference between LH/LH and RH/LH ground states is shown in Fig. 3 (orange-dotted) as a function of the number of molecules N . Clearly, the correlated ground and excited states illustrate a quick increase of the discriminating effect – the center-point of chiral polaritonics. The ground-state discrimination scales linear in N for moderate coupling and continues to scale as \sqrt{N} in the deep ultra-strong coupling domain (see SI). Both limits are consistent with the observation by Riso et al.⁵⁹

The small value of ξ for typical molecules translates into an overall small eigenvalue difference that scales on resonance approximately with $\sqrt{N}\tilde{g}\tilde{\xi}$. While $\sqrt{N}\tilde{g}$ can reach a sizeable fraction of the excitation energy, a major limi-

tation to be fought here is the commonly weak chirality. In order to leverage chiral polaritonics for enantiomer selectivity, it seems thus essential to either magnify the magnetic components or establish a protocol that can exploit the small energetic differences.

The latter follows closely the still open question for the origin of homochirality, i.e., how could a minute energetic imbalance between the enantiomers result in the real-world dominance of a given handedness.⁸⁸ Among the frequently discussed options are autocatalytic processes that turn a small imbalance into a substantial excess.⁸⁹ Chiral polaritonics could not just explore a similar path but serve as a sensitive framework to further elucidate the origin of homochirality.

The former approach on the other hand would propose the design of a cavity that would compensate for the small $\tilde{\xi}$. The discriminating factor $1 + \tilde{\xi}\lambda$ is in our purely transversal cavity bound by the small size of $\tilde{\xi}$ as $|\lambda| = 1$ is fixed by $Z\mathbf{H} = -i\lambda\mathbf{E}$. The latter, however, no longer holds in subwavelength cavities, where the field has a significant longitudinal component. In (non-chiral) plasmonic nanocavities, for example, $|Z\mathbf{H}| \ll |\mathbf{E}|$. Thus, the challenge could be addressed by designing a compact chiral nanocavity, whose quasi-normal mode is dominated by the longitudinal magnetic field, $|Z\mathbf{H}| \gg |\mathbf{E}|$, and maintains a chiral character expressed by a non-zero local chirality density $C(\mathbf{r})$.

We developed a new analytical model describing non-perturbative interaction of an ensemble of chiral molecules with a common chiral optical mode, i.e., a resonator that supports only optical modes with a given handedness. The model illustrates that a chiral cavity can be used to selectively couple to molecules of a specific handedness and thus provides means to discriminate enantiomers from a racemic. Such a chiral discriminating effect can be observed in all eigenstates of the strongly hybridized light-matter system and exists in absence of any pumping, i.e., in the dark cavity. How strong left and right-handed enantiomer can be distinguished is proportional to $\sqrt{N}g\xi$. While $\sqrt{N}g$ can become sizeable, the degree of chirality satisfies

typically $\xi \ll 1$ which currently limits the capability for chiral recognition. Possible strategies to exploit field enhancement techniques⁵⁷ in combined optical and plasmonic systems⁹⁰ might pave a way to enhance the recognition capabilities. It should be noted that this simple, accurately controllable and easily realizable system breaks a discrete symmetry with possibly wide and yet unforeseen ramifications. Chiral polaritonics contributes, even at this early stage, an exciting perspective to further elucidate homochirality. The intuitive analytical model and perspective put forward in this letter will foster this new domain on the intersection of cavity QED, chiral chemistry, biology and nanophotonics.

Acknowledgement We thank Göran Johansson, Maxim Gorkunov, and Timur Shegai for stimulating discussions. C.S. acknowledges support from the Swedish Research Council (VR) through Grant No. 2016-06059. D.G.B. acknowledges support from the Russian Science Foundation (21-72-00051) and BASIS foundation (Grant No. 22-1-3-2-1).

References

- (1) Garcia-Vidal, F. J.; Ciuti, C.; Ebbesen, T. W. Manipulating matter by strong coupling to vacuum fields. *Science* **2021**, *373*, eabd0336.
- (2) Simpkins, B. S.; Dunkelberger, A. D.; Owrutsky, J. C. Mode-specific chemistry through vibrational strong coupling (or A wish come true). *The Journal of Physical Chemistry C* **2021**, *125*, 19081–19087.
- (3) Sidler, D.; Ruggenthaler, M.; Schäfer, C.; Ronca, E.; Rubio, A. A perspective on ab initio modeling of polaritonic chemistry: The role of non-equilibrium effects and quantum collectivity. *The Journal of Chemical Physics* **2022**, *156*, 230901.
- (4) Forn-Díaz, P.; Lamata, L.; Rico, E.; Kono, J.; Solano, E. Ultrastrong coupling regimes of light-matter interaction. *Rev. Mod. Phys.* **2019**, *91*, 025005.
- (5) Kockum, A. F.; Miranowicz, A.; De Liberato, S.; Savasta, S.; Nori, F. Ultrastrong coupling between light and matter. *Nat. Rev. Phys.* **2019**, *1*, 19.
- (6) Mennucci, B.; Corni, S. Multiscale modelling of photoinduced processes in composite systems. *Nature Reviews Chemistry* **2019**, *3*, 315–330.
- (7) Luk, H. L.; Feist, J.; Toppari, J. J.; Groenhof, G. Multiscale Molecular Dynamics Simulations of Polaritonic Chemistry. *Journal of chemical theory and computation* **2017**, *13*, 4324–4335.
- (8) Fregoni, J.; Haugland, T. S.; Pipolo, S.; Giovannini, T.; Koch, H.; Corni, S. Strong coupling between localized surface plasmons and molecules by coupled cluster theory. *Nano Letters* **2021**, *21*, 6664–6670.
- (9) Bajoni, D.; Senellart, P.; Wertz, E.; Sagnes, I.; Miard, A.; Lemaître, A.; Bloch, J. Polariton laser using single micropillar GaAs- GaAlAs semiconductor cavities. *Physical review letters* **2008**, *100*, 047401.
- (10) Chikkaraddy, R.; de Nijs, B.; Benz, F.; Barrow, S. J.; Scherman, O. A.; Rosta, E.; Demetriadou, A.; Fox, P.; Hess, O.; Baumberg, J. J. Single-molecule strong coupling at room temperature in plasmonic nanocavities. *Nature* **2016**, *535*, 127–130.
- (11) Wang, D.; Kelkar, H.; Martin-Cano, D.; Utikal, T.; Götzinger, S.; Sandoghdar, V. Coherent Coupling of a Single Molecule to a Scanning Fabry-Perot Microcavity. *Phys. Rev. X* **2017**, *7*, 021014.
- (12) Baranov, D. G.; Munkhbat, B.; Zhukova, E.; Bisht, A.; Canales, A.; Rousseaux, B.; Johansson, G.; Antosiewicz, T. J.; Shegai, T. Ultrastrong coupling between nanoparticle plasmons and cavity photons at ambient conditions. *Nat. Commun.* **2020**, *11*, 2715.

- (13) Hübener, H.; De Giovannini, U.; Schäfer, C.; Andberger, J.; Ruggenthaler, M.; Faist, J.; Rubio, A. Engineering quantum materials with chiral optical cavities. *Nature materials* **2021**, *20*, 438–442.
- (14) Gubbin, C. R.; De Liberato, S. Optical Nonlocality in Polar Dielectrics. *Phys. Rev. X* **2020**, *10*, 021027.
- (15) Thomas, P. A.; Menghrajani, K. S.; Barnes, W. L. Cavity-Free Ultrastrong Light-Matter Coupling. *The Journal of Physical Chemistry Letters* **2021**, *12*, 6914–6918.
- (16) Coles, D. M.; Somaschi, N.; Michetti, P.; Clark, C.; Lagoudakis, P. G.; Savvidis, P. G.; Lidzey, D. G. Polariton-mediated energy transfer between organic dyes in a strongly coupled optical microcavity. *Nat. Mater.* **2014**, *13*, 712–719.
- (17) Orgiu, E.; George, J.; Hutchison, J. A.; Devaux, E.; Dayen, J. F.; Doudin, B.; Stellacci, F.; Genet, C.; Schachenmayer, J.; Genes, C. et al. Conductivity in organic semiconductors hybridized with the vacuum field. *Nat. Mater.* **2015**, *14*, 1123–1129.
- (18) Zhong, X.; Chervy, T.; Zhang, L.; Thomas, A.; George, J.; Genet, C.; Hutchison, J. A.; Ebbesen, T. W. Energy Transfer between Spatially Separated Entangled Molecules. *Angew. Chem. Int. Ed.* **2017**, *56*, 9034–9038.
- (19) Schäfer, C.; Ruggenthaler, M.; Appel, H.; Rubio, A. Modification of excitation and charge transfer in cavity quantum-electrodynamical chemistry. *Proceedings of the National Academy of Sciences* **2019**, *116*, 4883–4892.
- (20) Du, M.; Martínez-Martínez, L. A.; Ribeiro, R. F.; Hu, Z.; Menon, V. M.; Yuen-Zhou, J. Theory for polariton-assisted remote energy transfer. *Chem. Sci.* **2018**, *9*, 6659–6669.
- (21) Hagenmüller, D.; Schütz, S.; Schachenmayer, J.; Genes, C.; Pupillo, G. Cavity-assisted mesoscopic transport of fermions: Coherent and dissipative dynamics. *Phys. Rev. B* **2018**, *97*, 205303.
- (22) Cohn, B.; Sufrin, S.; Basu, A.; Chuntunov, L. Vibrational Polaritons in Disordered Molecular Ensembles. *The Journal of Physical Chemistry Letters* **2022**, *13*, 8369–8375.
- (23) Hutchison, J. A.; Schwartz, T.; Genet, C.; Devaux, E.; Ebbesen, T. W. Modifying Chemical Landscapes by Coupling to Vacuum Fields. *Angew. Chem. Int. Ed.* **2012**, *51*, 1592–1596.
- (24) Thomas, A.; Lethuillier-Karl, L.; Nagarajan, K.; Vergauwe, R. M.; George, J.; Chervy, T.; Shalabney, A.; Devaux, E.; Genet, C.; Moran, J. et al. Tilting a ground-state reactivity landscape by vibrational strong coupling. *Science* **2019**, *363*, 615–619.
- (25) Singh, J.; Lather, J.; George, J. Solvent Dependence on Cooperative Vibrational Strong Coupling and Cavity Catalysis. *ChemRxiv* **2022**,
- (26) Imperatore, M. V.; Asbury, J. B.; Giebink, N. C. Reproducibility of cavity-enhanced chemical reaction rates in the vibrational strong coupling regime. *The Journal of Chemical Physics* **2021**, *154*, 191103.
- (27) Schäfer, C.; Flick, J.; Ronca, E.; Narang, P.; Rubio, A. Shining light on the microscopic resonant mechanism responsible for cavity-mediated chemical reactivity. *Nature Communications* **2022**, *13*, 1–9.
- (28) Schäfer, C. Polaritonic Chemistry from First Principles via Embedding Radiation Reaction. *The Journal of Physical Chemistry Letters* **2022**, *13*, 6905–6911.
- (29) Li, T. E.; Nitzan, A.; Subotnik, J. E. Collective vibrational strong coupling effects

- on molecular vibrational relaxation and energy transfer: Numerical insights via cavity molecular dynamics simulations. *Angewandte Chemie* **2021**, *133*, 15661–15668.
- (30) Li, X.; Mandal, A.; Huo, P. Cavity frequency-dependent theory for vibrational polariton chemistry. *Nat. Commun.* **2021**, *12*, 1315.
- (31) Galego, J.; Garcia-Vidal, F. J.; Feist, J. Suppressing photochemical reactions with quantized light fields. *Nat. Commun.* **2016**, *7*, 13841.
- (32) Munkhbat, B.; Wersäll, M.; Baranov, D. G.; Antosiewicz, T. J.; Shegai, T. Suppression of photo-oxidation of organic chromophores by strong coupling to plasmonic nanoantennas. *Sci. Adv.* **2018**, *4*, eaas9552.
- (33) Groenhof, G.; Climent, C.; Feist, J.; Morozov, D.; Toppari, J. J. Tracking Polariton Relaxation with Multiscale Molecular Dynamics Simulations. *J. Phys. Chem. Lett.* **2019**, *10*, 5476–5483.
- (34) Kowalewski, M.; Bennett, K.; Mukamel, S. Cavity femtochemistry: Manipulating nonadiabatic dynamics at avoided crossings. *The journal of physical chemistry letters* **2016**, *7*, 2050–2054.
- (35) Vendrell, O. Collective Jahn-Teller Interactions through Light-Matter Coupling in a Cavity. *Phys. Rev. Lett.* **2018**, *121*, 253001.
- (36) Fábri, C.; Halász, G. J.; Vibók, Á. Probing Light-Induced Conical Intersections by Monitoring Multidimensional Polaritonic Surfaces. *The Journal of Physical Chemistry Letters* **2021**, *13*, 1172–1179.
- (37) Li, T. E.; Tao, Z.; Hammes-Schiffer, S. Semiclassical Real-Time Nuclear-Electronic Orbital Dynamics for Molecular Polaritons: Unified Theory of Electronic and Vibrational Strong Couplings. *Journal of Chemical Theory and Computation* **2022**, *18*, 2774–2784.
- (38) Fischer, E. W.; Anders, J.; Saalfrank, P. Cavity-altered thermal isomerization rates and dynamical resonant localization in vibro-polaritonic chemistry. *The Journal of Chemical Physics* **2022**, *156*, 154305.
- (39) Deng, H.; Weihs, G.; Snoke, D.; Bloch, J.; Yamamoto, Y. Polariton lasing vs. photon lasing in a semiconductor microcavity. *Proceedings of the National Academy of Sciences* **2003**, *100*, 15318–15323.
- (40) Kéna-Cohen, S.; Forrest, S. Room-temperature polariton lasing in an organic single-crystal microcavity. *Nature Photonics* **2010**, *4*, 371–375.
- (41) Sliotzky, M.; Liu, X.; Menon, V. M.; Forrest, S. R. Room temperature Frenkel-Wannier-Mott hybridization of degenerate excitons in a strongly coupled microcavity. *Phys. Rev. Lett.* **2014**, *112*, 076401.
- (42) Latini, S.; Shin, D.; Sato, S. A.; Schäfer, C.; De Giovannini, U.; Hübener, H.; Rubio, A. The ferroelectric photo ground state of SrTiO₃: Cavity materials engineering. *Proceedings of the National Academy of Sciences* **2021**, *118*, e2105618118.
- (43) Flick, J.; Welakuh, D. M.; Ruggenthaler, M.; Appel, H.; Rubio, A. Light-Matter Response in Nonrelativistic Quantum Electrodynamics. *ACS Photonics* **2019**, *6*, 2757–2778.
- (44) Schlawin, F.; Kennes, D. M.; Sentef, M. A. Cavity quantum materials. *Applied Physics Reviews* **2022**, *9*, 011312.
- (45) Schäfer, C.; Johansson, G. Shortcut to Self-Consistent Light-Matter Interaction and Realistic Spectra from First Principles. *Phys. Rev. Lett.* **2022**, *128*, 156402.
- (46) Lentrodt, D.; Heeg, K. P.; Keitel, C. H.; Evers, J. Ab initio quantum models for

- thin-film x-ray cavity QED. *Phys. Rev. Research* **2020**, *2*, 023396.
- (47) Debnath, A.; Rubio, A. Entangled photon assisted multidimensional nonlinear optics of exciton–polaritons. *Journal of Applied Physics* **2020**, *128*, 113102.
- (48) Lindell, I.; Sihvola, A.; Tretyakov, S.; Vitanen, A. *Electromagnetic waves in chiral and Bi-isotropic media*; Artech House, 2018; p 332.
- (49) Barron, L. D. *Molecular Light Scattering and Optical Activity*; Cambridge University Press, 2004; p 443.
- (50) Condon, E. U. Theories of Optical Rotatory Power. *Reviews of Modern Physics* **1937**, *9*, 432–457.
- (51) Kelvin, W. T. B. *The Molecular Tactics of a Crystal*; Robert Boyle lecture; Clarendon Press, 1894.
- (52) Weiskopf, R. B.; Nau, C.; Strichartz, G. R. Drug Chirality in Anesthesia. *Anesthesiology* **2002**, *97*, 497–502.
- (53) Calcaterra, A.; D’Acquarica, I. The market of chiral drugs: Chiral switches versus de novo enantiomerically pure compounds. *Journal of Pharmaceutical and Biomedical Analysis* **2018**, *147*, 323–340.
- (54) Scriba, G. K. Chiral recognition in separation science – an update. *Journal of Chromatography A* **2016**, *1467*, 56–78.
- (55) Weinberger, R. In *Practical Capillary Electrophoresis (Second Edition)*, second edition ed.; Weinberger, R., Ed.; Academic Press: San Diego, 2000; pp 139–208.
- (56) Roberts, J. D.; Caserio, M. C. *Basic principles of organic chemistry*; WA Benjamin, Inc., 1977.
- (57) Govorov, A. O.; Fan, Z.; Hernandez, P.; Slocik, J. M.; Naik, R. R. Theory of circular dichroism of nanomaterials comprising chiral molecules and nanocrystals: Plasmon enhancement, dipole interactions, and dielectric effects. *Nano Letters* **2010**, *10*, 1374–1382.
- (58) Mauro, L.; Fregoni, J.; Feist, J.; Avriller, R. Chiral Discrimination in Helicity-Preserving Fabry-Pérot Cavities. *arXiv preprint arXiv:2209.00402* **2022**,
- (59) Riso, R. R.; Grazioli, L.; Ronca, E.; Giovannini, T.; Koch, H. Strong coupling in chiral cavities: nonperturbative framework for enantiomer discrimination. *arXiv preprint arXiv:2209.01987* **2022**,
- (60) Voronin, K.; Taradin, A. S.; Gorkunov, M. V.; Baranov, D. G. Single-handedness chiral optical cavities. *ACS Photonics* **2022**, *9*, 2652–2659.
- (61) Schäfer, C.; Buchholz, F.; Penz, M.; Ruggenthaler, M.; Rubio, A. Making ab initio QED functional (s): Nonperturbative and photon-free effective frameworks for strong light–matter coupling. *Proceedings of the National Academy of Sciences* **2021**, *118*, e2110464118.
- (62) Haugland, T. S.; Ronca, E.; Kjønstad, E. F.; Rubio, A.; Koch, H. Coupled cluster theory for molecular polaritons: Changing ground and excited states. *Phys. Rev. X* **2020**, *10*, 041043.
- (63) Haugland, T. S.; Schäfer, C.; Ronca, E.; Rubio, A.; Koch, H. Intermolecular interactions in optical cavities: An ab initio QED study. *J. Chem. Phys.* **2021**, *154*, 094113.
- (64) Flick, J.; Ruggenthaler, M.; Appel, H.; Rubio, A. Atoms and molecules in cavities, from weak to strong coupling in quantum-electrodynamics (QED) chemistry. *Proceedings of the National Academy of Sciences* **2017**, *114*, 3026–3034.
- (65) Ruggenthaler, M.; Tancogne-Dejean, N.; Flick, J.; Appel, H.; Rubio, A. From

- a quantum-electrodynamical light–matter description to novel spectroscopies. *Nat. Rev. Chem.* **2018**, *2*, 0118.
- (66) Mason, S. F. *Optical activity and chiral discrimination*; Springer Science & Business Media, 2013; Vol. 48.
- (67) Li, X.; Shapiro, M. Theory of the optical spatial separation of racemic mixtures of chiral molecules. *The Journal of chemical physics* **2010**, *132*, 194315.
- (68) Forbes, K. A.; Andrews, D. L. Orbital angular momentum of twisted light: chirality and optical activity. *Journal of Physics: Photonics* **2021**, *3*, 022007.
- (69) Babiker, M.; Power, E. A.; Thirunamachandran, T. On a generalization of the Power–Zienau–Woolley transformation in quantum electrodynamics and atomic field equations. *Proceedings of the Royal Society of London. A. Mathematical and Physical Sciences* **1974**, *338*, 235–249.
- (70) Craig, I. R.; Manolopoulos, D. E. Quantum statistics and classical mechanics: Real time correlation functions from ring polymer molecular dynamics. *J. Chem. Phys.* **2004**, *121*, 3368–3373.
- (71) Forbes, K. A. Role of magnetic and diamagnetic interactions in molecular optics and scattering. *Phys. Rev. A* **2018**, *97*, 053832.
- (72) Andrews, D. L.; Jones, G. A.; Salam, A.; Woolley, R. G. Perspective: Quantum Hamiltonians for optical interactions. *The Journal of chemical physics* **2018**, *148*, 040901.
- (73) Schäfer, C.; Ruggenthaler, M.; Rokaj, V.; Rubio, A. Relevance of the quadratic diamagnetic and self-polarization terms in cavity quantum electrodynamics. *ACS Photonics* **2020**, *7*, 975–990.
- (74) Power, E. A.; Thirunamachandran, T. Quantum electrodynamics in a cavity. *Phys. Rev. A* **1982**, *25*, 2473.
- (75) Viehmann, O.; von Delft, J.; Marquardt, F. Superradiant phase transitions and the standard description of circuit QED. *Phys. Rev. Lett.* **2011**, *107*, 113602.
- (76) Ashida, Y.; İmamoglu, A. m. c.; Faist, J.; Jaksch, D.; Cavalleri, A.; Demler, E. Quantum Electrodynamic Control of Matter: Cavity-Enhanced Ferroelectric Phase Transition. *Phys. Rev. X* **2020**, *10*, 041027.
- (77) Lenk, K.; Li, J.; Werner, P.; Eckstein, M. Collective theory for an interacting solid in a single-mode cavity. *arXiv preprint arXiv:2205.05559* **2022**,
- (78) De Bernardis, D.; Jaako, T.; Rabl, P. Cavity quantum electrodynamics in the non-perturbative regime. *Phys. Rev. A* **2018**, *97*, 043820.
- (79) Nataf, P.; Champel, T.; Blatter, G.; Basko, D. M. Rashba Cavity QED: A Route Towards the Superradiant Quantum Phase Transition. *Phys. Rev. Lett.* **2019**, *123*, 207402.
- (80) Andolina, G. M.; Pellegrino, F. M. D.; Giovannetti, V.; MacDonald, A. H.; Polini, M. Theory of photon condensation in a spatially varying electromagnetic field. *Phys. Rev. B* **2020**, *102*, 125137.
- (81) Baranov, D. G.; Munkhbat, B.; Länk, N. O.; Verre, R.; Käll, M.; Shegai, T. Circular dichroism mode splitting and bounds to its enhancement with cavity-plasmon-polaritons. *Nanophotonics* **2020**, *9*, 283–293.
- (82) Semnani, B.; Flannery, J.; Al Maruf, R.; Bajcsy, M. Spin-preserving chiral photonic crystal mirror. *Light: Science and Applications* **2020**, *9*, 23.
- (83) Fernandez-Corbaton, I.; Fruhnert, M.; Rockstuhl, C. Objects of maximum electromagnetic chirality. *Physical Review X* **2016**, *6*, 031013.

- (84) Schäfer, C.; Ruggenthaler, M.; Rubio, A. Ab initio nonrelativistic quantum electrodynamics: Bridging quantum chemistry and quantum optics from weak to strong coupling. *Phys. Rev. A* **2018**, *98*, 043801.
- (85) Hopfield, J. J. Theory of the Contribution of Excitons to the Complex Dielectric Constant of Crystals. *Phys. Rev.* **1958**, *112*, 1555–1567.
- (86) George, J.; Chervy, T.; Shalabney, A.; Devaux, E.; Hiura, H.; Genet, C.; Ebbesen, T. W. Multiple Rabi Splittings under Ultrastrong Vibrational Coupling. *Phys. Rev. Lett.* **2016**, *117*, 153601.
- (87) Todorov, Y.; Sirtori, C. Intersubband polaritons in the electrical dipole gauge. *Phys. Rev. B* **2012**, *85*, 045304.
- (88) So Much More to Know. *Science* **2005**, *309*, 78–102.
- (89) Blackmond, D. G. Asymmetric autocatalysis and its implications for the origin of homochirality. *Proceedings of the National Academy of Sciences* **2004**, *101*, 5732–5736.
- (90) Hertzog, M.; Munkhbat, B.; Baranov, D.; Shegai, T.; Börjesson, K. Enhancing Vibrational Light–Matter Coupling Strength beyond the Molecular Concentration Limit Using Plasmonic Arrays. *Nano letters* **2021**, *21*, 1320–1326.

Supplemental Information to Chiral Polaritonics: Analytic Solutions, Intuition and its Use

Christian Schäfer^{1,*} and Denis G. Baranov^{2,†}

¹*MC2 Department, Chalmers University of Technology, Sweden*

²*Center for Photonics and 2D Materials,*

Moscow Institute of Physics and Technology, Dolgoprudny 141700, Russia

Abstract

The Supplemental Information provides an extended derivation of the chiral Hopfield and Tavis-Cummings model and an alternative derivation of the chiral Hopfield model in which the self-polarization terms are partially cancelled which results in an instability of the chiral system.

FIELDS OF A STANDING CHIRAL WAVE

In the following we obtain explicit expressions for the electric and magnetic fields of a chiral standing wave describing the optical mode of a single-handedness optical cavity. We begin with the case of a standing wave formed by two counter-propagating circularly polarized plane waves. The field of a monochromatic circularly polarized plane wave propagating through air in the positive direction of the z axis takes the form ($e^{-i\omega t}$ time dependence for the harmonic field is assumed):

$$\mathbf{E}_{+z}^\lambda(\mathbf{r}) = \frac{\mathcal{E}}{\sqrt{2}} \begin{pmatrix} 1 \\ i\lambda \\ 0 \end{pmatrix} e^{ikz}, \quad Z\mathbf{H}_{+z}^\lambda(\mathbf{r}) = -i\lambda\mathbf{E}_{+z}^\lambda(\mathbf{r}), \quad (\text{S1})$$

where $\lambda = \pm 1$ denotes the handedness of the wave, $k = \omega/c$, and \mathcal{E} has units of electric field. Correspondingly, the fields of a wave travelling in the negative direction of the z axis takes the form:

$$\mathbf{E}_{-z}^\lambda(\mathbf{r}) = \frac{\mathcal{E}}{\sqrt{2}} \begin{pmatrix} 1 \\ -i\lambda \\ 0 \end{pmatrix} e^{-ikz}, \quad Z\mathbf{H}_{-z}^\lambda(\mathbf{r}) = -i\lambda\mathbf{E}_{-z}^\lambda(\mathbf{r}). \quad (\text{S2})$$

The fields of a "vertical" standing wave take the form:

$$\mathbf{E}_{\mathbf{k}_\parallel=0}^\lambda = \frac{\mathbf{E}_{+z}^\lambda + \mathbf{E}_{-z}^\lambda}{\sqrt{2}} = \mathcal{E} \begin{pmatrix} \cos kz \\ -\lambda \sin kz \\ 0 \end{pmatrix}, \quad Z\mathbf{H}_{\mathbf{k}_\parallel=0}^\lambda = -i\lambda\mathbf{E}_{\mathbf{k}_\parallel=0}^\lambda(\mathbf{r}). \quad (\text{S3})$$

Now consider a pair of circularly polarized plane waves with a given handedness λ both propagating with a fixed in-plane momentum \mathbf{k}_\parallel (in-plane with respect to the vertical axis of the cavity) and opposite vertical component of the wave vector $\pm k_z \hat{\mathbf{z}}$. Without loss of generality let us assume $\mathbf{k}_\parallel = k_x \hat{\mathbf{x}}$ with $k_x = k \sin \theta$ and $k_z = \pm k \cos \theta$. Electric fields take the form:

$$\mathbf{E}_{+z,\mathbf{k}_\parallel}^\lambda(\mathbf{r}) = \frac{\mathcal{E}}{\sqrt{2}} \begin{pmatrix} \cos \theta \\ i\lambda \\ -\sin \theta \end{pmatrix} e^{ik_z z + ik_x x}, \quad \mathbf{E}_{-z,\mathbf{k}_\parallel}^\lambda(\mathbf{r}) = \frac{\mathcal{E}}{\sqrt{2}} \begin{pmatrix} \cos \theta \\ -i\lambda \\ +\sin \theta \end{pmatrix} e^{-ik_z z + ik_x x} \quad (\text{S4})$$

The z -dependent electric field of the combination of the two waves with the common \mathbf{k}_{\parallel} takes the form:

$$\mathbf{E}_{\mathbf{k}_{\parallel}}^{\lambda}(\mathbf{r}) = \mathcal{E} \begin{pmatrix} \cos \theta \cos k_z z \\ -\lambda \sin k_z z \\ -i \sin \theta \sin k_z z \end{pmatrix} e^{ik_x x}. \quad (\text{S5})$$

Magnetic field of the chiral standing wave with handedness λ follows from the electric field:

$$Z\mathbf{H}_{\mathbf{k}_{\parallel}}^{\lambda} = -i\lambda\mathbf{E}_{\mathbf{k}_{\parallel}}^{\lambda}. \quad (\text{S6})$$

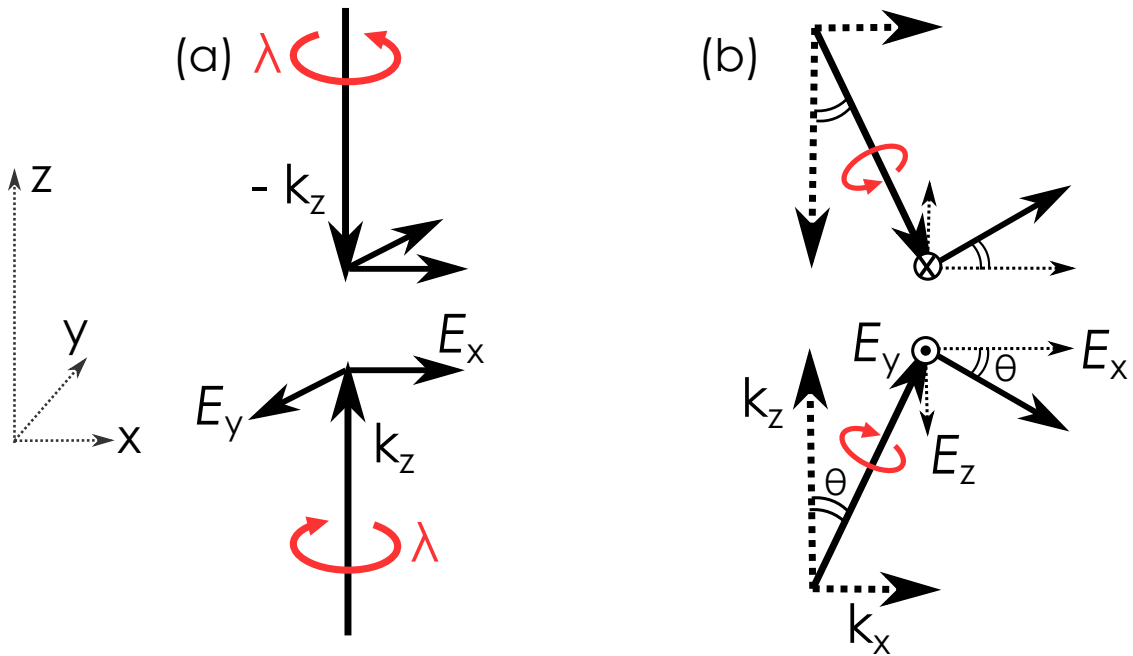


FIG. S1. Geometry of a chiral standing wave.

DERIVING THE CHIRAL HOPFIELD AND TAVIS-CUMMINGS MODELS

We start with the chiral standing fields that are derived from the generic mode expansion

$$\begin{aligned}\hat{\mathbf{D}}_{\perp}(\mathbf{r}) &= i \sum_{\mathbf{k},\lambda} \sqrt{\frac{\hbar ck \epsilon_0}{2V}} \left(\epsilon_{\mathbf{k}\lambda} e^{i\mathbf{k}\cdot\mathbf{r}} \hat{a}_{\mathbf{k}\lambda} - \epsilon_{\mathbf{k}\lambda}^* e^{-i\mathbf{k}\cdot\mathbf{r}} \hat{a}_{\mathbf{k}\lambda}^{\dagger} \right), \\ \hat{\mathbf{B}}(\mathbf{r}) &= i \frac{1}{c} \sum_{\mathbf{k},\lambda} \sqrt{\frac{\hbar ck}{2\epsilon_0 V}} \left(\beta_{\mathbf{k}\lambda} e^{i\mathbf{k}\cdot\mathbf{r}} \hat{a}_{\mathbf{k}\lambda} - \beta_{\mathbf{k}\lambda}^* e^{-i\mathbf{k}\cdot\mathbf{r}} \hat{a}_{\mathbf{k}\lambda}^{\dagger} \right).\end{aligned}$$

Following the explanations in the main text, 'upwards' and 'downwards' propagating fields are superimposed as

$$\begin{aligned}\hat{\mathbf{D}}_{\perp}^{\lambda}(\mathbf{r}) &= \sum_{\mathbf{k},\lambda} \hat{\mathbf{D}}_{\mathbf{k},\perp}^{\lambda}(\mathbf{r}), \\ \hat{\mathbf{D}}_{\perp}^{\lambda}(\mathbf{r}) &= \sum_k (\hat{\mathbf{D}}_{+k,\perp}^{\lambda}(\mathbf{r}) + \hat{\mathbf{D}}_{-k,\perp}^{\lambda}(\mathbf{r})) / \sqrt{2},\end{aligned}$$

with $\hat{a}_{+k_z,\lambda} = \hat{a}_{-k_z,\lambda}$ and $\epsilon_{\pm k,\lambda} = \frac{1}{\sqrt{2}}(1, \pm i\lambda, 0)^T$. One obtains

$$\hat{\mathbf{D}}_{\perp}^{\lambda}(\mathbf{r}) = - \sum_{k>0} \sqrt{\frac{\epsilon_0}{V}} \tilde{\epsilon}_k^{\lambda}(z) \hat{p}_{k,\lambda},$$

with $\tilde{\epsilon}_k^{\lambda}(z) = (\cos(kz), -\lambda \sin(kz), 0)^T$ and $\hat{p}_{k,\lambda} = -i\sqrt{\hbar ck/2}(\hat{a}_{\mathbf{k},\lambda} - \hat{a}_{\mathbf{k},\lambda}^{\dagger})$, $\hat{q}_{k,\lambda} = \sqrt{\hbar/2ck}(\hat{a}_{\mathbf{k},\lambda} + \hat{a}_{\mathbf{k},\lambda}^{\dagger})$. The same procedure is applied to the magnetic fields where now however $\beta_{\mathbf{k},\lambda} = -i\lambda\epsilon_{\mathbf{k},\lambda}$ such that the chiral standing magnetic field features the additional λ

$$\hat{\mathbf{B}}_{\lambda}(\mathbf{r}) = \sum_{k>0} \sqrt{k^2/\epsilon_0 V} \lambda \tilde{\epsilon}_k^{\lambda}(z) \hat{q}_{k,\lambda}.$$

Considering that $\nabla \times \tilde{\epsilon}_k^{\lambda}(z) = \lambda k \tilde{\epsilon}_k^{\lambda}(z)$, it is easily validated that those fields fulfill Maxwell's equations of motion and contribute the common photonic energy $\sum_{k>0} \hbar\omega_k (\hat{a}^{\dagger}\hat{a} + \frac{1}{2})$ per handedness λ .

We will assume in the following that only a single mode couples substantially to the ensemble of chiral molecules, a reasonable approximation for most cavity realizations that should be however relaxed if the inter-molecular distances become much larger than the wavelength of the electromagnetic standing field. Explicitly expressing all components in

the Hamiltonian leads to

$$\begin{aligned}
\hat{H} &= \sum_n \hat{H}_{M,n} + \frac{1}{2\varepsilon_0 V} \left[\sum_n \tilde{\varepsilon}_k^\lambda(z) \cdot \hat{\boldsymbol{\mu}}_n \right]^2 + \frac{1}{2} \hat{p}_k^2 \\
&+ \frac{1}{2} \left[\omega_k^2 + \sum_{n=1}^{N_{mol}} \sum_{i,j=1}^3 2\hat{\chi}_{n,ij}^m \frac{k^2}{\varepsilon_0 V} \tilde{\varepsilon}_{k,i}^\lambda(z) \tilde{\varepsilon}_{k,j}^\lambda(z) \right] \hat{q}_k^2 \\
&+ \sum_n \sqrt{\frac{1}{\varepsilon_0 V}} \left[\tilde{\varepsilon}_k^\lambda(z) \cdot \hat{\boldsymbol{\mu}}_n + \sum_{a,b \in \{x,y,z\}} \hat{Q}_{ab,n} \nabla_{a,n} \tilde{\varepsilon}_{k,b}^\lambda(z) \right] \hat{p}_k \\
&- \sum_n \sqrt{\frac{k^2}{\varepsilon_0 V}} \lambda \tilde{\varepsilon}_k^\lambda(z) \cdot \hat{\mathbf{m}}_n \hat{q}_k.
\end{aligned} \tag{S7}$$

The self-magnetization term mediated via $\hat{\chi}_{n,ij}^m$ represents our first obstacle since it combines operators to cubic order, thus going beyond the otherwise quadratic form. In combination with the self-polarization term, the self-magnetization ensures gauge invariance and the stability of the combined system which renders it essential for any future developments of *ab initio* cavity QED. As we strive for a simple analytical solution, we will assume a parametric dependence $\hat{\chi}_{n,ij}^m \approx \chi_{n,ij}^m$ such that $\bar{\omega}_k^2 = \omega_k^2 \left[1 + 2 \sum_n \sum_{i,j=1}^3 \chi_{n,ij}^m \tilde{\varepsilon}_{k,i}^\lambda(z) \tilde{\varepsilon}_{k,j}^\lambda(z) / (c^2 \varepsilon_0 V) \right]$ characterized the effective photonic frequency. While this correction is inherently small ($\propto 1/c^2$), it should be noted that it scales linear in the number of molecules. As $\chi_{n,ij}^m$ is rarely even mentioned and to the best of our knowledge never considered, it remains an open problem to specify its dynamic value. It is however possible to set the value for $\bar{\omega}_k$ in relation to the systems characteristic solution. Using the sum-rule $\langle m | [\hat{p}_k, [\hat{H}, \hat{p}_k]] | m \rangle = 2 \sum_n (E_n - E_m) |\langle m | \hat{p}_k | n \rangle|^2$ with eigenvalues E_m and eigenstates $|m\rangle$ provides $\bar{\omega}_k^2 = 2 \sum_n (E_n - E_m) / \hbar^2 |\langle m | \hat{p}_k | n \rangle|^2 \quad \forall m$. We will formally retain the self-magnetization term but ultimately ignore its influence on the visualization. It should be noted that the following model features a magnetic instability for sizeable particle number and ξ if $\bar{\omega}_k$ is not adjusted accordingly. We will limit our discussion to the stable domain, i.e., where phase transitions are absent. Importantly, any *ab initio* calculation that includes the flexibility to change the electric/nuclear structure should include *all* components [1, 2].

Transition dipole moments

We will illustrate the identification and relation of the transition moment for the two-level approximation in the following. The corresponding Hopfield model, featuring an identification with harmonic oscillators instead, is derived analogously. We disregard permanent

dipole moments for brevity

$$\hat{\boldsymbol{\mu}}_n \rightarrow (\boldsymbol{\mu}_{10}^n \hat{\sigma}_+ + \boldsymbol{\mu}_{01}^n \hat{\sigma}_-), \quad (\text{S8})$$

$$\hat{\mathbf{m}}_n \rightarrow (\mathbf{m}_{10}^n \hat{\sigma}_+ + \mathbf{m}_{01}^n \hat{\sigma}_-), \quad (\text{S9})$$

where the matrix elements of the transition dipole moment (TDM) operators are calculated according to

$$\boldsymbol{\mu}_{01} = \langle 0 | \hat{\boldsymbol{\mu}} | 1 \rangle, \quad \mathbf{m}_{01} = \langle 0 | \hat{\mathbf{m}} | 1 \rangle, \quad (\text{S10})$$

and the lowering and raising operators of the TLS are given by the standard expressions

$$\sigma_+ = |1\rangle\langle 0|, \quad \sigma_- = \sigma_+^\dagger = |0\rangle\langle 1|. \quad (\text{S11})$$

Without the loss of generality, the matrix element of the electric TDM operator may be assumed real-valued, $\boldsymbol{\mu}_{01} = \boldsymbol{\mu}_{01}^*$.

Let us establish the general relationship between transition dipole moments of a two-level quantum emitter. For a bi-isotropic molecule with parallel electric and magnetic transition dipole moments this equation takes the simple form [3]:

$$\mathbf{m}_{01}^n = -ic\xi \boldsymbol{\mu}_{01}^n, \quad (\text{S12})$$

with $\xi = \pm 1$ corresponding to LH (+1) and RH (-1) emitters, respectively. Correspondingly, the magnetic dipole moment operator becomes $\hat{\mathbf{m}} = ic\xi(\boldsymbol{\mu}_{01}^* \hat{\sigma}_+ - \boldsymbol{\mu}_{01} \hat{\sigma}_-)$. The above relationship between the TDMs of a chiral emitter is consistent with the chirality definition of a classical monochromatic dipolar source [4]. Let us now look for a more general tensorial expression that would relate the transition dipole moments of an anisotropic molecular emitter.

Three Euler angles unambiguously describe the orientation of any rigid body (such as a molecule) in space. Similarly, a pair of non-collinear vectors $\boldsymbol{\mu}_{01}$ and \mathbf{m}_{01} hard-wired to the molecule would work. But $\boldsymbol{\mu}_{01}$ and \mathbf{m}_{01} are not independent themselves, and must satisfy a molecule-specific characteristic equation. First let us fix the orientation of the electric dipole moment of the molecule $\boldsymbol{\mu}_{01}$. This vector needs to be mapped into the magnetic transition dipole moment \mathbf{m}_{01} . Suppose this mapping is performed by a dyad $\overset{\leftrightarrow}{\xi}$, as illustrated in Fig. S2. This dyad cannot be an arbitrary linear transformation: the action of $\overset{\leftrightarrow}{\xi}$ on $\boldsymbol{\mu}_{01}$ must be invariant with respect to an arbitrary rotation of the molecule. Thus, $\overset{\leftrightarrow}{\xi}$ must be a product

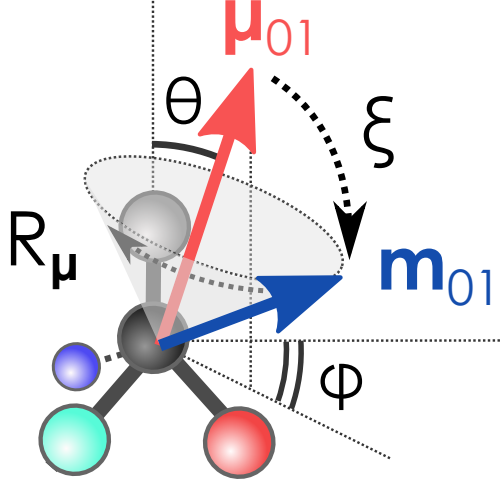


FIG. S2. Illustration of the relationship between the electric and magnetic transition dipole moments in a generic molecular emitter. The orientation of the transition electric dipole moment $\boldsymbol{\mu}_{01}$ associated with the molecule can be described by two angles θ, φ in a local spherical coordinates system. $\overleftrightarrow{\xi}$ describes a unitary mapping $\boldsymbol{\mu} \rightarrow \mathbf{m}$. For a given orientation of the electric dipole moment $\boldsymbol{\mu}_{01}$, all allowed positions of \mathbf{m}_{01} occupy a circle denoted by the shaded area. This additional mapping is accomplished by the rotation of the molecule around $\boldsymbol{\mu}_{01}$, which is described by $R_{\boldsymbol{\mu}}$.

of an orthogonal linear transformation \overleftrightarrow{U} in \mathbb{R}^3 and scaling by a complex number s :

$$\overleftrightarrow{\xi} = s \cdot \overleftrightarrow{U}. \quad (\text{S13})$$

We can further specify its form by incorporating two rotations into the spatial orientation of $\boldsymbol{\mu}_{01}$. Choosing a linearly-polarized transition electric dipole moment $\boldsymbol{\mu}_{01}$ is equivalent to fixing two Euler angles of the molecular orientation, leaving an arbitrary rotation around $\boldsymbol{\mu}_{01}$. For example, we can parameterize the electric TDM by the polar and azimuthal angles in the spherical coordinate system:

$$\boldsymbol{\mu}_{01} = |\boldsymbol{\mu}| \begin{pmatrix} \sin \theta \cos \varphi \\ \sin \theta \sin \varphi \\ \cos \theta \end{pmatrix}. \quad (\text{S14})$$

A given tensor $\overleftrightarrow{\xi}$ will map a given electric dipole moment $\boldsymbol{\mu}_{01}$ into another fixed vector. However, given a fixed $\boldsymbol{\mu}_{01}$ all allowed positions of \mathbf{m}_{01} occupy an entire circle in \mathbb{R}^3 . Thus, mapping $\boldsymbol{\mu}_{01} \rightarrow \mathbf{m}_{01}$ must be parameterized by an additional angle describing rotations of

the molecule around $\boldsymbol{\mu}_{01}$ (see Fig. S2). The sought for mapping thus can be written as:

$$\mathbf{m}_{01} = -ic\overset{\leftrightarrow}{R}_\mu(\delta)\overset{\leftrightarrow}{\xi}\boldsymbol{\mu}_{01}, \quad (\text{S15})$$

where $\overset{\leftrightarrow}{R}_\mu(\delta)$ is the rotation matrix that describes rotation of the molecule around $\boldsymbol{\mu}_{01}$ by an angle δ . The mapping parameterized by three angles $(\theta, \varphi, \delta)$ in Eq. S15 encompasses all possible orientations of the molecule, which allows us to average any characteristic of the coupled system (such as the coupling constant) over molecular orientation.

Let us now establish the constraints imposed on $\overset{\leftrightarrow}{\xi}$ by reciprocity. The linear relationship between induced electric and magnetic dipole moments of a polarizable subwavelength object and incident monochromatic field can be written as:

$$\begin{pmatrix} \mathbf{p} \\ \mathbf{m} \end{pmatrix} = \begin{pmatrix} \varepsilon_0\overset{\leftrightarrow}{\alpha}_e & \overset{\leftrightarrow}{\alpha}_{em}/c \\ \varepsilon_0c\overset{\leftrightarrow}{\alpha}_{me} & \overset{\leftrightarrow}{\alpha}_m \end{pmatrix} \begin{pmatrix} \mathbf{E} \\ \mathbf{H} \end{pmatrix}, \quad (\text{S16})$$

where $\overset{\leftrightarrow}{\varepsilon}$, $\overset{\leftrightarrow}{\mu}$, $\overset{\leftrightarrow}{\alpha}_{em}$, and $\overset{\leftrightarrow}{\alpha}_{me}$ are all rank-2 3×3 tensors with units of volume.

We limit our treatment to the class of reciprocal media; polarizabilities of any reciprocal particle are subject to Onsager-Casimir relations [5]:

$$\begin{aligned} \overset{\leftrightarrow}{\alpha}_e &= \overset{\leftrightarrow}{\alpha}_e^T, \\ \overset{\leftrightarrow}{\alpha}_m &= \overset{\leftrightarrow}{\alpha}_m^T, \\ \overset{\leftrightarrow}{\alpha}_{em} &= -\overset{\leftrightarrow}{\alpha}_{me}^T. \end{aligned} \quad (\text{S17})$$

This criterion allows us to decompose the magneto-electric coupling tensors into reciprocal ('R') and non-reciprocal ('NR') components:

$$\overset{\leftrightarrow}{\alpha}_{em} = \overset{\leftrightarrow}{\alpha}_{em}^{(NR)} + \overset{\leftrightarrow}{\alpha}_{em}^{(R)} \equiv \overset{\leftrightarrow}{\chi} + i\overset{\leftrightarrow}{\kappa}, \quad (\text{S18})$$

$$\overset{\leftrightarrow}{\alpha}_{me} = \overset{\leftrightarrow}{\alpha}_{me}^{(NR)} + \overset{\leftrightarrow}{\alpha}_{me}^{(R)} \equiv \overset{\leftrightarrow}{\chi} - i\overset{\leftrightarrow}{\kappa}. \quad (\text{S19})$$

where the reciprocal part is presented by $\overset{\leftrightarrow}{\kappa}$:

$$\overset{\leftrightarrow}{\kappa} = \frac{\overset{\leftrightarrow}{\alpha}_{em} - \overset{\leftrightarrow}{\alpha}_{me}^T}{2i}, \quad (\text{S20})$$

and the non-reciprocal part is presented by

$$\overset{\leftrightarrow}{\chi} = \frac{\overset{\leftrightarrow}{\alpha}_{em} + \overset{\leftrightarrow}{\alpha}_{me}^T}{2}. \quad (\text{S21})$$

Obviously, if $\overleftrightarrow{\chi} = 0$, then $\overleftrightarrow{\alpha}_{em} = -\overleftrightarrow{\alpha}_{me}^T$, and the reciprocity criterion is satisfied. It is self-explanatory that the reciprocal part of magneto-electric polarizability is responsible for effects that respect reciprocity.

Atomic polarizabilities of the elementary two-level system with arbitrary transition dipole moments $\boldsymbol{\mu}$ and \mathbf{m} can be written as:

$$\overleftrightarrow{\alpha}_e = \frac{\boldsymbol{\mu}_{01} \otimes \boldsymbol{\mu}_{01}^*}{\hbar\varepsilon_0} \frac{1}{\omega_0 - \omega - i\gamma/2}, \quad \overleftrightarrow{\alpha}_m = \frac{\mathbf{m}_{01} \otimes \mathbf{m}_{01}^*}{\hbar\varepsilon_0 c^2} \frac{1}{\omega_0 - \omega - i\gamma/2}, \quad (\text{S22})$$

$$\overleftrightarrow{\alpha}_{em} = \frac{\boldsymbol{\mu}_{01} \otimes \mathbf{m}_{01}^*}{\hbar\varepsilon_0 c} \frac{1}{\omega_0 - \omega - i\gamma/2}, \quad \overleftrightarrow{\alpha}_{me} = \frac{\mathbf{m}_{01} \otimes \boldsymbol{\mu}_{01}^*}{\hbar\varepsilon_0 c} \frac{1}{\omega_0 - \omega - i\gamma/2}. \quad (\text{S23})$$

Equations S22 suggest that for $\overleftrightarrow{\alpha}_e$ and $\overleftrightarrow{\alpha}_m$ to comply with Casimir-Onsager relations, Eq. S17, $\boldsymbol{\mu}_{01}$ and \mathbf{m}_{01} must be real-valued vectors (up to an arbitrary global phase $e^{i\phi}$), thus describing linearly-polarized transitions. One can easily see that plugging $\mathbf{m}_{01} = -ic\xi\boldsymbol{\mu}_{01}$ (Eq. S12) into the above expressions yields $\overleftrightarrow{\alpha}_{em} = -\overleftrightarrow{\alpha}_{me}^T$ and $\overleftrightarrow{\chi} = 0$.

Now let us utilize Eq. S15 and for brevity work with the numerator of the full expression in Eq. S23:

$$\begin{aligned} \overleftrightarrow{\alpha}_{em} \propto \boldsymbol{\mu}_{01} \otimes \mathbf{m}_{01}^* &\equiv \boldsymbol{\mu}_{01} \mathbf{m}_{01}^\dagger = \boldsymbol{\mu}_{01} \left(-ic \overleftrightarrow{R}_\mu \overleftrightarrow{\xi} \boldsymbol{\mu}_{01} \right)^\dagger \\ &= \boldsymbol{\mu}_{01} \left(-ic \boldsymbol{\mu}_{01}^T (\overleftrightarrow{R}_\mu \overleftrightarrow{\xi})^T \right)^* = ic \boldsymbol{\mu}_{01} \boldsymbol{\mu}_{01}^\dagger (\overleftrightarrow{R}_\mu \overleftrightarrow{\xi})^\dagger. \end{aligned} \quad (\text{S24})$$

Similarly, for α_{me} we obtain:

$$\overleftrightarrow{\alpha}_{me} \propto \mathbf{m}_{01} \otimes \boldsymbol{\mu}_{01}^* \equiv \mathbf{m}_{01} \boldsymbol{\mu}_{01}^\dagger = -ic \left(\overleftrightarrow{R}_\mu \overleftrightarrow{\xi} \right) \boldsymbol{\mu}_{01} \boldsymbol{\mu}_{01}^\dagger. \quad (\text{S25})$$

Transposing the latter, assuming without the loss of generality the real-valued $\boldsymbol{\mu}_{01}$ and inserting into the Casimir-Onsager relation, we get:

$$\overleftrightarrow{\alpha}_{em} + \overleftrightarrow{\alpha}_{me}^T \propto ic \boldsymbol{\mu}_{01} \boldsymbol{\mu}_{01}^\dagger [(\overleftrightarrow{R}_\mu \overleftrightarrow{\xi})^\dagger - (\overleftrightarrow{R}_\mu \overleftrightarrow{\xi})^T] = 0. \quad (\text{S26})$$

Since $\overleftrightarrow{R}_\mu$ is a real-valued orthogonal matrix, the latter implies that for a reciprocal bi-anisotropic two-level emitter $\overleftrightarrow{\xi}$ must be real-valued:

$$\boxed{\Im[\overleftrightarrow{\xi}] = 0.} \quad (\text{S27})$$

In other words, the scaling factor s of the transformation is real-valued, $\Im[s] = 0$.

For now, let us assume that the transition dipole moments are related by the simple expression with a scalar ξ , Eq. S12. Using this compact relation between electric and

magnetic moments allows us to combine electric dipole, electric quadrupole and magnetic dipole into a single compact expression (assuming $\boldsymbol{\mu}_{10}^n = \boldsymbol{\mu}_{10}^{n,*}$ and $Q_{ab,n}^{10} = Q_{ab,n}^{01}$, $\mathbf{Q}_n = Q_{ab,n}^{10} \nabla_a \mathbf{e}_b$):

$$\begin{aligned} \hat{H} = & \sum_n \hat{H}_{M,n} + \frac{1}{2\varepsilon_0 V} \left[\sum_n \tilde{\varepsilon}_k^\lambda(z) \cdot \boldsymbol{\mu}_{01}^n (\sigma_n^+ + \sigma_n^-) \right]^2 + \hbar \bar{\omega}_k \left(\hat{a}^\dagger \hat{a} + \frac{1}{2} \right) \\ & - i \sum_n \bar{g}_n \left[(\sigma_n^+ + \sigma_n^-) (\hat{a} - \hat{a}^\dagger) - \bar{\xi}_n \lambda (\sigma_n^+ - \sigma_n^-) (\hat{a} + \hat{a}^\dagger) \right] \end{aligned} \quad (\text{S28})$$

where

$$\bar{g}_n = \sqrt{\frac{\hbar \bar{\omega}_k}{2\varepsilon_0 V}} (\boldsymbol{\mu}_{10}^n + \mathbf{Q}_n) \cdot \tilde{\varepsilon}_k^\lambda(z) \quad (\text{S29})$$

and

$$\bar{\xi}_n = \frac{\omega_k}{\bar{\omega}_k} \frac{\boldsymbol{\mu}_{10}^n \cdot \tilde{\varepsilon}_k^\lambda(z)}{(\boldsymbol{\mu}_{10}^n + \mathbf{Q}_n) \cdot \tilde{\varepsilon}_k^\lambda(z)} \xi. \quad (\text{S30})$$

Tavis-Cummings models – a hint at the effective coupling strength

Let us here introduce the common matter-representation of two-level models, discard the self-polarization term and all counter-rotating terms ($\propto \hat{a} \hat{\sigma}^- \approx 0$ and similar). We obtain the strongly simplified chiral Tavis-Cummings Hamiltonian:

$$\hat{H}_{CTC} = \sum_n \hbar \omega_m \hat{\sigma}_n^+ \hat{\sigma}_n^- + \hbar \bar{\omega}_k \left(\hat{a}^\dagger \hat{a} + \frac{1}{2} \right) - i \hbar \sum_n \bar{g}_n (1 + \bar{\xi}_n \lambda) \left[\hat{\sigma}_n^+ \hat{a} - \hat{\sigma}_n^- \hat{a}^\dagger \right] \quad (\text{S31})$$

that shows explicitly that the effective interaction strength is proportional to $\bar{g}_n (1 + \bar{\xi}_n \lambda)$. A chiral emitter that features the same handedness as the cavity will couple stronger to the mode. In the extreme case that $\bar{\xi}_n = \pm 1$, the mismatched enantiomer will entirely decouple from the mode. The above chiral Tavis-Cummings model could be solved analytically in the same way as any Tavis-Cummings model, i.e, by limiting ourselves to the single-excitation subspace and introducing collective spin-operators. Here, we will focus on the Hopfield model that includes also the counter-rotating and self-polarization terms that can lead to sizeable renormalizations for large N .

Chiral Hopfield model

In contrast to the Dicke and Tavis-Cummings models with a two-level approximation, the Hopfield approach is based on representing the material in terms of harmonic oscillators

which allows for an analytic solution also in the ultra-strong coupling domain. The first polariton manifold is identical in the single-excitation + strong-coupling regime. Our Chiral Hopfield Hamiltonian takes the form of $N + 1$ coupled harmonic oscillators

$$\begin{aligned}\hat{H} &= \sum_n \hbar\omega_n(\hat{b}_n^\dagger\hat{b}_n + \frac{1}{2}) + \hbar\bar{\omega}_k(\hat{a}^\dagger\hat{a} + \frac{1}{2}) \\ &- i\hbar\sum_n \bar{g}_n [(\hat{b}_n^\dagger + \hat{b}_n)(\hat{a} - \hat{a}^\dagger) + \bar{\xi}_n\lambda(\hat{b}_n^\dagger - \hat{b}_n)(\hat{a} + \hat{a}^\dagger)] \\ &+ \frac{1}{2\varepsilon_0V} \left[\sum_n \tilde{\varepsilon}_k^\lambda(z) \cdot \boldsymbol{\mu}_{01}^n(\hat{b}_n^\dagger + \hat{b}_n) \right]^2.\end{aligned}\quad (\text{S32})$$

The transition-dipole moments are related to the optical oscillator strength of the harmonic model. Assuming identical molecules, it is convenient to introduce the Fourier-representation for the molecular ensemble

$$\hat{B}_{\mathbf{k}}^\dagger = \frac{1}{\sqrt{N}} \sum_n e^{i\mathbf{k}\cdot\mathbf{r}_n} \hat{b}_n^\dagger, \quad \hat{b}_n^\dagger = \frac{1}{\sqrt{N}} \sum_{\mathbf{k}} e^{-i\mathbf{k}\cdot\mathbf{r}_n} \hat{B}_{\mathbf{k}}^\dagger \quad (\text{S33})$$

such that the collective operators are represented by bright $\sum_n \hat{b}^\dagger = \sqrt{N}\hat{B}_{k=0}^\dagger$ and dark states

$$\begin{aligned}\hat{H} &\approx \hbar\omega_m(\hat{B}_{k=0}^\dagger\hat{B}_{k=0} + \frac{1}{2}) + \hbar\omega_m \sum_{k \neq 0} \hat{B}_k^\dagger\hat{B}_k + (N-1)\frac{\hbar\omega_m}{2} + \hbar\bar{\omega}_k(\hat{a}^\dagger\hat{a} + \frac{1}{2}) \\ &- i\hbar\sqrt{N}\bar{g} [(\hat{B}_{k=0}^\dagger + \hat{B}_{k=0})(\hat{a} - \hat{a}^\dagger) + \bar{\xi}\lambda(\hat{B}_{k=0}^\dagger - \hat{B}_{k=0})(\hat{a} + \hat{a}^\dagger)] \\ &+ \frac{N}{2\varepsilon_0V} \left[\tilde{\varepsilon}_k^\lambda(z) \cdot \boldsymbol{\mu}_{01}(\hat{B}_{k=0}^\dagger + \hat{B}_{k=0}) \right]^2.\end{aligned}\quad (\text{S34})$$

Disregarding the dark states $\hbar\omega_m \sum_{k \neq 0} \hat{B}_k^\dagger\hat{B}_k$ and their vacuum-fluctuations $(N-1)\frac{\hbar\omega_m}{2}$, the self-polarization term can be absorbed into an adjusted matter frequency of the bright states $\tilde{\omega}_m^2 = \omega_m^2 + N\frac{2\omega_m}{\hbar\varepsilon_0V}(\tilde{\varepsilon}_k^\lambda(z) \cdot \boldsymbol{\mu}_{01})^2$ which results in

$$\begin{aligned}\hat{H} &= \hbar\tilde{\omega}_m(\hat{B}_{k=0}^\dagger\hat{B}_{k=0} + \frac{1}{2}) + \hbar\bar{\omega}_k(\hat{a}^\dagger\hat{a} + \frac{1}{2}) \\ &- i\hbar\sqrt{N}\tilde{g} [(\hat{B}_{k=0}^\dagger + \hat{B}_{k=0})(\hat{a} - \hat{a}^\dagger) + \tilde{\xi}\lambda(\hat{B}_{k=0}^\dagger - \hat{B}_{k=0})(\hat{a} + \hat{a}^\dagger)].\end{aligned}\quad (\text{S35})$$

where $\tilde{g} = \sqrt{\frac{\hbar\bar{\omega}_k\omega_m}{2\varepsilon_0V\omega_m}}(\boldsymbol{\mu}_{01} + \mathbf{Q}_n) \cdot \tilde{\varepsilon}_k^\lambda(z)$ and $\tilde{\xi} = \frac{\tilde{\omega}_m\omega_k}{\omega_m\bar{\omega}_k} \frac{\boldsymbol{\mu}_{01} \cdot \tilde{\varepsilon}_k^\lambda(z)}{(\boldsymbol{\mu}_{01} + \mathbf{Q}) \cdot \tilde{\varepsilon}_k^\lambda(z)} \xi$ are the renormalized effective coupling strength and chirality factor.

We can diagonalize Eq. (S35) by following the standard Hopfield [6, 7] procedure, i.e., defining the polaritonic operator $\hat{\Pi} = x\hat{a} + y\hat{a}^\dagger + z\hat{B}_{k=0} + u\hat{B}_{k=0}^\dagger$ that fulfills the eigenvalue equation $[\hat{H}, \hat{\Pi}] = \hbar\Omega\hat{\Pi}$ with the normalization condition $|x|^2 - |y|^2 + |z|^2 - |u|^2 = 1$. We

obtain the polaritonic frequencies from

$$\begin{vmatrix} -\bar{\omega}_k - \Omega & 0 & (1 + \tilde{\xi}\lambda)i\sqrt{N}\tilde{g} & -(1 - \tilde{\xi}\lambda)i\sqrt{N}\tilde{g} \\ 0 & \bar{\omega}_k - \Omega & -(1 - \tilde{\xi}\lambda)i\sqrt{N}\tilde{g} & (1 + \tilde{\xi}\lambda)i\sqrt{N}\tilde{g} \\ -(1 + \tilde{\xi}\lambda)i\sqrt{N}\tilde{g} & -(1 - \tilde{\xi}\lambda)i\sqrt{N}\tilde{g} & -\tilde{\omega}_m - \Omega & 0 \\ -(1 - \tilde{\xi}\lambda)i\sqrt{N}\tilde{g} & -(1 + \tilde{\xi}\lambda)i\sqrt{N}\tilde{g} & 0 & \tilde{\omega}_m - \Omega \end{vmatrix} = 0 \quad (\text{S36})$$

as real and positive solutions

$$\Omega_{\pm} = \frac{1}{\sqrt{2}} \sqrt{\bar{\omega}_k^2 + \tilde{\omega}_m^2 + 8\tilde{\xi}\lambda N\tilde{g}^2 \pm \sqrt{[\omega_k^2 - \tilde{\omega}_m^2]^2 + 16N\tilde{g}^2(\bar{\omega}_k + \tilde{\omega}_m\tilde{\xi}\lambda)(\bar{\omega}_k\tilde{\xi}\lambda + \tilde{\omega}_m)}}. \quad (\text{S37})$$

The corresponding eigenvectors encode in $|x|^2 - |y|^2$ the matter contribution and in $|z|^2 - |u|^2$ the photonic contribution to the polaritonic states.

Generic alignment and its influence on chiral recognition

Let us briefly examine the more general case where the electric and magnetic transition dipole moments are arbitrarily oriented. In this case, they are related by Eq. S22 with $\overset{\leftrightarrow}{\xi} = s\overset{\leftrightarrow}{U}$ where s is real-valued and $\overset{\leftrightarrow}{U}$ is an orthogonal transformation.

The orientation average is described by the energy-conserving squared coupling element:

$$\langle |g|^2 \rangle \propto \frac{1}{4\pi} \int_0^{2\pi} d\phi \int_0^\pi d\theta \sin(\theta) |\sqrt{N}\tilde{\varepsilon} \cdot (1 + \lambda\overset{\leftrightarrow}{\xi})\boldsymbol{\mu}_{01}|^2 \quad (\text{S38})$$

proportional to the combined electric plus magnetic moments. Expanding the dot product

$$\begin{aligned} |\tilde{\varepsilon} \cdot (1 + \lambda\overset{\leftrightarrow}{\xi})\boldsymbol{\mu}_{01}|^2 &= \cos^2\theta |(1 + \lambda\overset{\leftrightarrow}{\xi})\boldsymbol{\mu}_{01}|^2 \\ &= \cos^2\theta \left(|\boldsymbol{\mu}_{01}|^2 + \langle \overset{\leftrightarrow}{\xi}\boldsymbol{\mu}_{01} | \overset{\leftrightarrow}{\xi}\boldsymbol{\mu}_{01} \rangle + 2\lambda \langle \boldsymbol{\mu}_{01} | \overset{\leftrightarrow}{\xi}\boldsymbol{\mu}_{01} \rangle \right) \end{aligned} \quad (\text{S39})$$

and utilizing $\overset{\leftrightarrow}{\xi} = s\overset{\leftrightarrow}{U}$, we obtain:

$$\begin{aligned} \langle |g|^2 \rangle &= \left| \sqrt{\frac{\hbar\bar{\omega}_k\omega_m}{2\varepsilon_0 V \tilde{\omega}_m \omega_m \bar{\omega}_k}} \tilde{\omega}_m \omega_k \sqrt{N} (1 + \lambda\overset{\leftrightarrow}{\xi}) \cdot \boldsymbol{\mu}_{01} \right|^2 \frac{1}{2} \int_0^\pi d\theta \sin(\theta) \cos^2(\theta) \\ &= \frac{N}{3} \frac{\hbar\tilde{\omega}_m\omega_k^2}{2\varepsilon_0 V \bar{\omega}_k\omega_m} |(1 + \lambda\overset{\leftrightarrow}{\xi}) \cdot \boldsymbol{\mu}_{01}|^2 \\ &= \frac{N}{3} \frac{\hbar\tilde{\omega}_m\omega_k^2}{2\varepsilon_0 V \bar{\omega}_k\omega_m} \left[(1 + s^2) |\boldsymbol{\mu}_{01}|^2 + 2\lambda s \Re \langle \boldsymbol{\mu}_{01} | \overset{\leftrightarrow}{U}\boldsymbol{\mu}_{01} \rangle \right]. \end{aligned} \quad (\text{S40})$$

In addition to chiral features that arise from the parallel components of the transition dipole moments, the emitters now also feature Omega-type magneto-electric coupling originating from the orthogonal components of the dipole moments. However, as we can easily see from the angular average, only the chiral components are discriminated by the cavity. Eq. (S40) clarifies that the chiral cavity will only distinguish the chiral components of the emitters. Take for example pure chirality with $\lambda = +1$ and (anti-)alignment $\boldsymbol{\mu} \parallel \mathbf{m}$ with $\overset{\leftrightarrow}{\xi} = \pm 1$, then $[(1 + s^2)|\boldsymbol{\mu}_{01}|^2 + 2\lambda s \Re\langle \boldsymbol{\mu}_{01} | \overset{\leftrightarrow}{U}_\xi \boldsymbol{\mu}_{01} \rangle] = (1 + 1 + 2(\pm 1))|\boldsymbol{\mu}_{01}|^2$, which is either 0 or $4|\boldsymbol{\mu}_{01}|^2$. However, for Ω -coupling $\langle \boldsymbol{\mu}_{01} | \overset{\leftrightarrow}{U} \boldsymbol{\mu}_{01} \rangle = 0$ and we obtain always $(1 + s^2)|\boldsymbol{\mu}_{01}|^2$. The transition-dipole moments still contribute constructively to the chiral coupling but there is no handedness selectivity left.

Influence of the self-magnetization

Let us illustrate briefly how the self-magnetization can influence our conclusions. First of all, it should be noticed that the dressing of the photonic frequency via χ^m is a factor $1/c^2$ smaller than the self-polarization effect on the matter frequency. However, even if we chose enormously large values, the effect is small as demonstrated in Fig. S3.

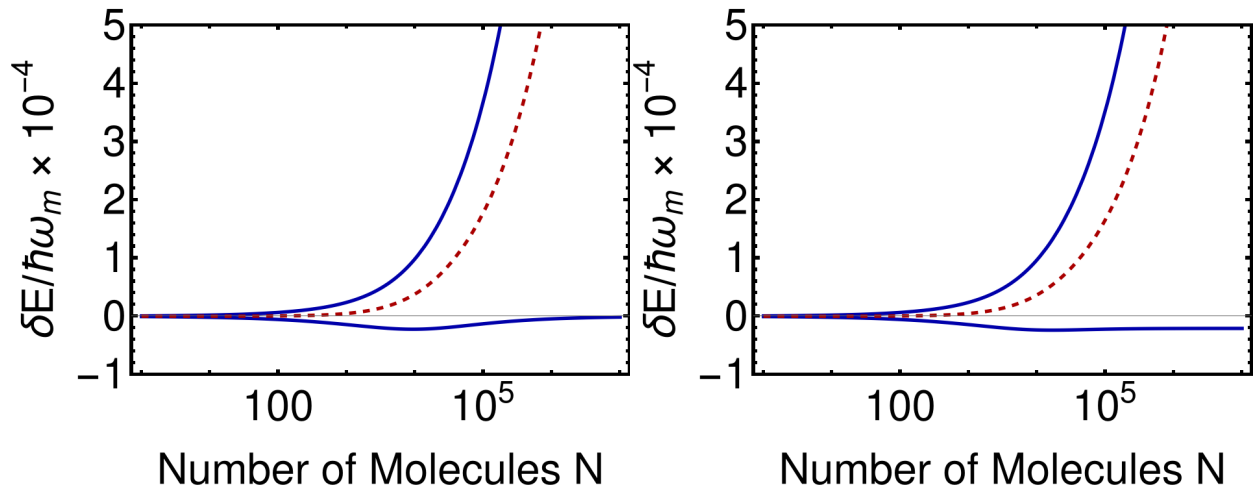


FIG. S3. Left, including a quite large self-magnetization of $\chi^m = \mu^2$. Right, using a vastly enhanced self-magnetization of $\chi^m = c^2 \mu^2$, so even if we compensate the $1/c^2$ factor, the effect of the self-magnetization is small. Interestingly, the large self-magnetization can even enhance the recognition capabilities in the lower polariton.

Extension to modes with non-zero in-plane momentum $k_x \neq 0$

Our previous derivations used the simplifying assumption of a cavity mode represented by a standing wave with $\mathbf{k} = \pm k\mathbf{e}_z$, which leads to compact and highly intuitive equations. A more generic description might allow for non-zero in-plane momentum $k_x \neq 0$, resulting in mixing of propagating waves and dark states. We will provide in the following a brief discussion what such an extension would look like and what changes are to be expected. We would like to emphasize that such an extended model would go more naturally with a many-mode description and present a straightforward generalization of our work.

A planar optical cavity, such as the one described in ref. [8], supports a continuous spectrum of resonant states that can be labeled by their in-plane momenta \mathbf{k}_\parallel . More sophisticated cavities, such as micro-domes, support more complex modes with in-plane contribution and non-Gaussian spot-distribution but we retain here with the simplified Fabry-Pérot set up. A minimal representation for the field of such cavity modes is given in Section *Fields of a standing chiral wave*. Cavity modes with $\mathbf{k}_\parallel \neq \mathbf{0}$ do maintain their single-handedness quality in a substantial range of in-plane wave vectors (incident angles) according to the findings of ref. [8], and thus are expected to feature similar energy spectra when coupled with chiral molecular emitters.

As before, we can expand the fields in its eigenmodes

$$\begin{aligned}\hat{\mathbf{D}}_\perp^\lambda(\mathbf{r}) &= i \sum_{\mathbf{k}} \sqrt{\frac{\hbar ck \varepsilon_0}{2V}} \left(\epsilon_{\mathbf{k}\lambda}(\mathbf{r}) \hat{a}_{\mathbf{k}\lambda} - \epsilon_{\mathbf{k}\lambda}^*(\mathbf{r}) \hat{a}_{\mathbf{k}\lambda}^\dagger \right), \\ \hat{\mathbf{B}}^\lambda(\mathbf{r}) &= i \frac{1}{c} \sum_{\mathbf{k}} \sqrt{\frac{\hbar ck}{2\varepsilon_0 V}} \left(\beta_{\mathbf{k}\lambda}(\mathbf{r}) \hat{a}_{\mathbf{k}\lambda} - \beta_{\mathbf{k}\lambda}^*(\mathbf{r}) \hat{a}_{\mathbf{k}\lambda}^\dagger \right)\end{aligned}$$

where $\epsilon_{\mathbf{k}\lambda}(\mathbf{r}) = \frac{1}{\sqrt{2}}(k_z/k, i\lambda, -k_x/k)^T e^{ik_z z + ik_x x}$ and $\beta_{\mathbf{k}\lambda}(\mathbf{r}) = -i\lambda \epsilon_{\mathbf{k}\lambda}(\mathbf{r})$ such that

$$\hat{\mathbf{B}}^\lambda(\mathbf{r}) = \frac{1}{c} \sum_{\mathbf{k}} \lambda \sqrt{\frac{\hbar ck}{2\varepsilon_0 V}} \left(\epsilon_{\mathbf{k}\lambda}(\mathbf{r}) \hat{a}_{\mathbf{k}\lambda} + \epsilon_{\mathbf{k}\lambda}^*(\mathbf{r}) \hat{a}_{\mathbf{k}\lambda}^\dagger \right).$$

We again restrict enforce the chiral standing wave in z-direction by $\hat{\mathbf{D}}_\perp^\lambda(\mathbf{r}) = \frac{1}{\sqrt{2}}(\hat{\mathbf{D}}_{\perp, k_z > 0}^\lambda(\mathbf{r}) + \hat{\mathbf{D}}_{\perp, k_z < 0}^\lambda(\mathbf{r}))$ which results with $\hat{a}_{k_x, k_z > 0, \lambda} = \hat{a}_{k_x, k_z < 0, \lambda}$ in

$$\begin{aligned}\hat{\mathbf{D}}_\perp^\lambda(\mathbf{r}) &= i \sum_{k_z > 0, k_x} \sqrt{\frac{\hbar ck \varepsilon_0}{2V}} \left(\tilde{\epsilon}_{\mathbf{k}\lambda}(\mathbf{r}) \hat{a}_{\mathbf{k}\lambda} - \tilde{\epsilon}_{\mathbf{k}\lambda}^*(\mathbf{r}) \hat{a}_{\mathbf{k}\lambda}^\dagger \right), \\ \hat{\mathbf{B}}^\lambda(\mathbf{r}) &= \frac{1}{c} \sum_{k_z > 0, k_x} \lambda \sqrt{\frac{\hbar ck}{2\varepsilon_0 V}} \left(\tilde{\epsilon}_{\mathbf{k}\lambda}(\mathbf{r}) \hat{a}_{\mathbf{k}\lambda} + \tilde{\epsilon}_{\mathbf{k}\lambda}^*(\mathbf{r}) \hat{a}_{\mathbf{k}\lambda}^\dagger \right)\end{aligned}$$

where $\tilde{\epsilon}_{\mathbf{k}\lambda}(\mathbf{r}) = (k_z/k \cos(k_z z), -\lambda \sin(k_z z), -ik_x/k \sin(k_z z))^T e^{ik_x x}$.

The projection of the matter degrees of freedom follows as before and the overall structure remains unchanged. As an example, we will derive the new Tavis-Cummings analogue, the Hopfield model can be obtain in analogy to the previous steps but the many-mode coupling renders the process more verbose. As before, we perform the rotating-wave approximation for the chiral Tavis-Cummings model and disregard all self-correction terms as well as quadrupole contributions to obtain

$$\begin{aligned} \hat{H}_{CTC}^\lambda &= \sum_n \hbar\omega_m \hat{\sigma}_n^+ \hat{\sigma}_n^- + \sum_{k_z > 0, k_x} \hbar\omega_{\mathbf{k}} (\hat{a}_{\mathbf{k}\lambda}^\dagger \hat{a}_{\mathbf{k}\lambda} + \frac{1}{2}) \\ &\quad - \sum_{n, k_z > 0, k_x} i \sqrt{\frac{\hbar ck}{2\epsilon_0 V}} \left[(\tilde{\epsilon}_{\mathbf{k}\lambda}(\mathbf{r}) \cdot \boldsymbol{\mu}_{01}^n \hat{\sigma}_n^+ \hat{a}_{\mathbf{k}\lambda} - h.a.) + \lambda (\tilde{\epsilon}_{\mathbf{k}\lambda}(\mathbf{r}) \overset{\leftrightarrow}{\xi}_n \boldsymbol{\mu}_{01}^n \hat{\sigma}_n^+ \hat{a}_{\mathbf{k}\lambda} - h.a.) \right]. \\ &= \sum_n \hbar\omega_m \hat{\sigma}_n^+ \hat{\sigma}_n^- + \sum_{k_z > 0, k_x} \hbar\omega_{\mathbf{k}} (\hat{a}_{\mathbf{k}\lambda}^\dagger \hat{a}_{\mathbf{k}\lambda} + \frac{1}{2}) - \sum_{n, k_z > 0, k_x} i \sqrt{\frac{\hbar ck}{2\epsilon_0 V}} \left[\tilde{\epsilon}_{\mathbf{k}\lambda}(\mathbf{r}) (1 + \lambda \overset{\leftrightarrow}{\xi}_n) \cdot \boldsymbol{\mu}_{01}^n \hat{\sigma}_n^+ \hat{a}_{\mathbf{k}\lambda} - h.a. \right]. \end{aligned}$$

We introduce again a Fourier-representation $\hat{\sigma}_n^+ = \frac{1}{\sqrt{N}} \sum_{\mathbf{K}} e^{-i\mathbf{K} \cdot \mathbf{r}_n} \hat{S}_{\mathbf{K}}^\dagger$ which implies a regular molecular distance along the x-axis $\mathbf{r}_n = \mathbf{e}_x \frac{2\pi n}{N}$ and assume identical couplings and frequencies. As $\sum_n e^{ik_x x_n} e^{-iK_x x_n} = N \delta(k_x - K_x)$, the chiral Tavis-Cummings Hamiltonian simplifies to

$$\begin{aligned} \hat{H}_{CTC}^\lambda &= \sum_K \hbar\omega_m \hat{S}_K^+ \hat{S}_K^- + \sum_{k_z > 0, k_x} \hbar\omega_{\mathbf{k}} (\hat{a}_{\mathbf{k}\lambda}^\dagger \hat{a}_{\mathbf{k}\lambda} + \frac{1}{2}) \\ &\quad - \sum_{k_z > 0, k_x} i \sqrt{N} \sqrt{\frac{\hbar ck}{2\epsilon_0 V}} \left[\tilde{\epsilon}_{\mathbf{k}\lambda}(z, x=0) (1 + \lambda \overset{\leftrightarrow}{\xi}) \cdot \boldsymbol{\mu}_{01} \hat{S}_{k_x}^+ \hat{a}_{\mathbf{k}\lambda} - h.a. \right]. \end{aligned} \tag{S41}$$

Comparison with Eq. (S31) clarifies that the chiral effect, i.e., $(1 + \lambda \overset{\leftrightarrow}{\xi})$, remains unchanged. An important difference is that for non-zero in-plane momentum, the coupling is not only to the mode $K_x = 0$ but also to higher momenta, similar to the standard Tavis-Cummings model as shown for example in Ref. [9].

CHIRAL HOPFIELD MODEL UNDER THE ASSUMPTION OF CANCELLING INSTANTANEOUS INTERMOLECULAR CONTRIBUTIONS

We provide here a derivation of the chiral Hopfield model under the assumption that the instantaneous intermolecular interactions cancel. Using the explicit form of the chiral fields, our starting point reads then

$$\begin{aligned}
\hat{H} &= \sum_n \left[\hat{H}_{M,n} + \frac{1}{2\varepsilon_0 V} (\tilde{\varepsilon}_k^\lambda(z) \cdot \hat{\boldsymbol{\mu}}_n)^2 \right] \\
&+ \frac{1}{2} \hat{p}_k^2 + \frac{1}{2} \left[\omega_k^2 + 2 \sum_n \hat{\chi}_{n,ij}^m \frac{k^2}{\varepsilon_0 V} \tilde{\varepsilon}_{k,i}^\lambda(z) \tilde{\varepsilon}_{k,j}^\lambda(z) \right] \hat{q}_k^2 \\
&+ \sum_n \sqrt{\frac{1}{\varepsilon_0 V}} \left[\tilde{\varepsilon}_k^\lambda(z) \cdot \hat{\boldsymbol{\mu}}_n + \sum_{a,b \in \{x,y,z\}} \hat{Q}_{ab,n} \nabla_{a,n} \tilde{\varepsilon}_{k,b}^\lambda(z) \right] \hat{p}_k \\
&- \sum_n \sqrt{\frac{k^2}{\varepsilon_0 V}} \lambda \tilde{\varepsilon}_k^\lambda(z) \cdot \hat{\mathbf{m}}_n \hat{q}_k
\end{aligned} \tag{S42}$$

where the only difference is that the self-polarization is local only.

We can follow the same steps as before and absorb the self-polarization into adjusted local matter frequencies $\tilde{\omega}_n^2 = \omega_n^2 + \frac{2m\omega_n}{\hbar\varepsilon_0 V} (\tilde{\varepsilon}_k^\lambda(z) \cdot \boldsymbol{\mu}_{10}^n)^2$ – notice the missing N. We obtain

$$\begin{aligned}
\hat{H} &= \sum_n \hbar \tilde{\omega}_n (\hat{b}_n^\dagger \hat{b}_n + \frac{1}{2}) + \hbar \bar{\omega}_k (\hat{a}^\dagger \hat{a} + \frac{1}{2}) \\
&- i\hbar \sum_n \tilde{g}_n \left[(\hat{b}_n^\dagger + \hat{b}_n) (\hat{a} - \hat{a}^\dagger) + \tilde{\xi}_n \lambda (\hat{b}_n^\dagger - \hat{b}_n) (\hat{a} + \hat{a}^\dagger) \right]
\end{aligned} \tag{S43}$$

where as before $\tilde{g}_n = \sqrt{\frac{\hbar \bar{\omega}_k \omega_n}{2\varepsilon_0 V \omega_n}} (\boldsymbol{\mu}_{10}^n + \mathbf{Q}_n) \cdot \tilde{\varepsilon}_k^\lambda(z)$ and $\tilde{\xi}_n = \frac{\tilde{\omega}_n \omega_k}{\omega_n \bar{\omega}_k} \frac{\boldsymbol{\mu}_{10}^n \cdot \tilde{\varepsilon}_k^\lambda(z)}{(\boldsymbol{\mu}_{10}^n + \mathbf{Q}_n) \cdot \tilde{\varepsilon}_k^\lambda(z)} \xi$ are the renormalized effective coupling strength and chirality factor. Introducing the Fourier-representation leads to

$$\begin{aligned}
\hat{H} &= \hbar \tilde{\omega}_m (\hat{B}_{k=0}^\dagger \hat{B}_{k=0} + \frac{1}{2}) + \hbar \tilde{\omega}_m \sum_{k \neq 0} \hat{B}_k^\dagger \hat{B}_k + (N-1) \frac{\hbar \tilde{\omega}_m}{2} + 2\hbar \bar{\omega}_k (\hat{a}^\dagger \hat{a} + \frac{1}{2}) \\
&- i\hbar \sqrt{N} \tilde{g} \left[(\hat{B}_{k=0}^\dagger + \hat{B}_{k=0}) (\hat{a} - \hat{a}^\dagger) + \tilde{\xi} \lambda (\hat{B}_{k=0}^\dagger - \hat{B}_{k=0}) (\hat{a} + \hat{a}^\dagger) \right].
\end{aligned} \tag{S44}$$

Importantly, also the dark states are now dressed by the self-polarization and $\tilde{\omega}_m$ does not depend on the number of molecules N. The analytic solution has the same form but deviates in $\tilde{\omega}_m$ which results in instabilities for large N.

Fig. S4 contrasts the two version (left without intersystem self-polarization) of the chiral Hopfield model and the associated instability.

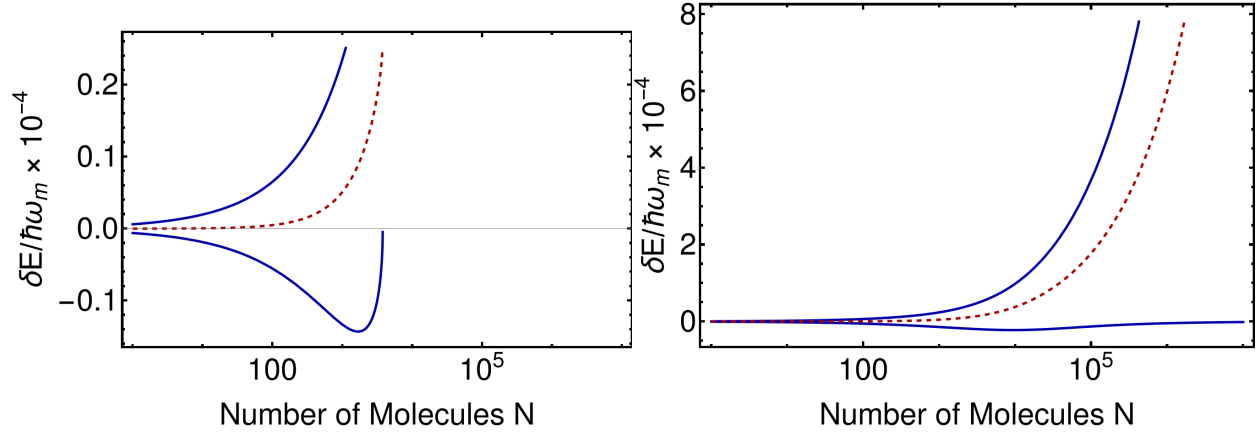


FIG. S4. N-scaling differences between left and right-handed chiral dye molecules as introduced in the paper. Left, without intersystem self-polarization, right, using full self-polarization and disregarding intermolecular Coulomb interactions (same as in main text). All parameters consistent with Fig. 3.

CONSISTENCY OF THE CHIRAL HOPFIELD MODEL IN THE ULTRA-STRONG COUPLING DOMAIN WITH *AB INITIO* CALCULATIONS

The Hopfield model has been shown to provide excellent results for vibrational strong coupling [10] and intersubband transitions [7]. It is not obvious that the same qualitative accuracy can be expected for the electronic subspace in atomic/molecular structures. However, recent work by Riso et al. [11] utilized an adjusted version of QED Coupled-cluster to estimate the discriminating strength of chiral fields on single and few molecules. They predict a \sqrt{N} behavior of the discriminating strength in the correlated ground-state (Fig. 5 of Ref. [11]) that is consistent with our observations shown in Fig. S5 if the coupling is deep within the ultra-strong coupling domain.

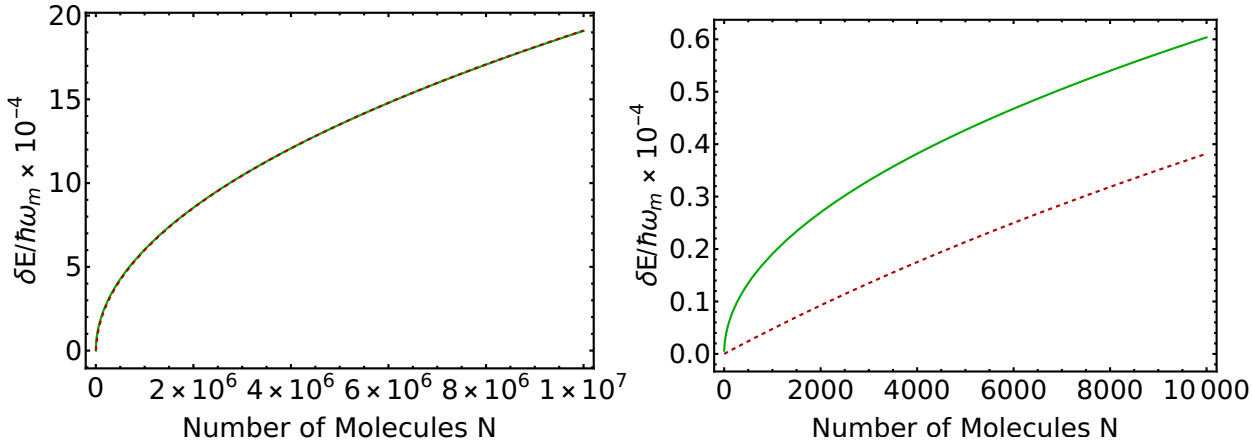


FIG. S5. N -scaling differences in the correlated ground-state between left and right-handed chiral dye molecules introduced in the paper (red-dashed). The green line following $6.5 \cdot 10^{-8} \sqrt{N}$ serves as guide to the eye. It is apparent that the large- N limit, which is equivalent with increasing the fundamental coupling strength, is dominated by a \sqrt{N} behavior that is consistent with the available literature. All parameters consistent with Fig. 3.

The overall trend of the polaritonic eigenvalues predicted by the Hopfield model is consistent with exact results for hydrogen as illustrated in Fig. S6.

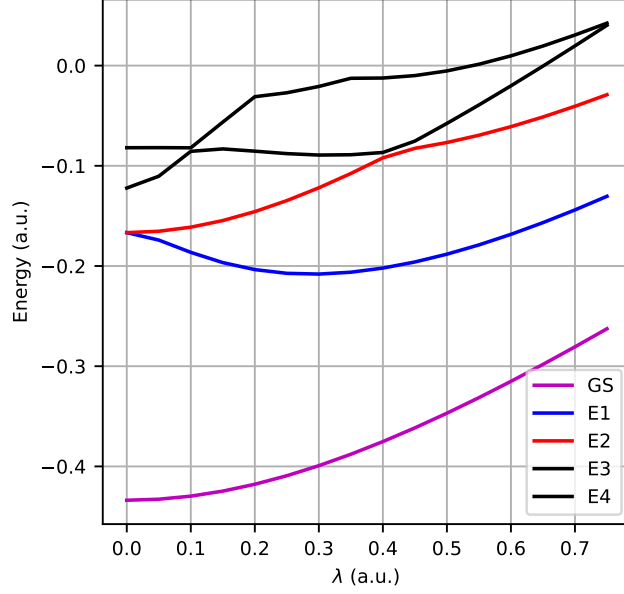


FIG. S6. Eigenvalues of two-dimensional soft-Coulomb hydrogen coupled in electric dipole approximation to a single cavity mode in resonance with the first matter-excitation. The exact solution uses a grid representation with 151×151 grid-points for hydrogen and 30 Fock-states for the cavity mode. We show the first 5 correlated eigenstates. In total, this amounts to a Hilbert space with 684030 states. Our simplified Hopfield model provides a similar trend (as long as the magnetic components do not dominate the coupling) and is therefore qualitatively consistent with exact solutions. The exact solution will naturally produce (avoided) crossings between higher excited states that are not included in our model but that do not influence the drawn conclusions.

* christian.schaefer.physics@gmail.com

† denis.baranov@phystech.edu

- [1] C. Schäfer, M. Ruggenthaler, V. Rokaj, and A. Rubio, *ACS Photonics* **7**, 975 (2020).
- [2] V. Rokaj, D. M. Welakuh, M. Ruggenthaler, and A. Rubio, *J. Phys. B* **51**, 034005 (2018).
- [3] E. U. Condon, *Reviews of Modern Physics* **9**, 432 (1937).
- [4] I. F. Corbaton, *Helicity and duality symmetry in light matter interactions: Theory and applications*, Ph.D. thesis, Macquarie University, Faculty of Science and Engineering (2014).
- [5] C. Caloz, A. Alu, S. Tretyakov, D. Sounas, K. Achouri, and Z.-L. Deck-Léger, *Physical Review Applied* **10**, 047001 (2018).
- [6] J. J. Hopfield, *Phys. Rev.* **112**, 1555 (1958).
- [7] Y. Todorov and C. Sirtori, *Phys. Rev. B* **85**, 045304 (2012).
- [8] K. Voronin, A. S. Taradin, M. V. Gorkunov, and D. G. Baranov, *ACS Photonics* **9**, 2652 (2022).
- [9] R. H. Tichauer, J. Feist, and G. Groenhof, *The Journal of Chemical Physics* **154**, 104112 (2021).
- [10] J. George, T. Chervy, A. Shalabney, E. Devaux, H. Hiura, C. Genet, and T. W. Ebbesen, *Phys. Rev. Lett.* **117**, 153601 (2016).
- [11] R. R. Riso, L. Grazioli, E. Ronca, T. Giovannini, and H. Koch, arXiv preprint arXiv:2209.01987 (2022).